The Next Generation Crystal Detectors for Future HEP Calorimeters

Ren-Yuan Zhu

California Institute of Technology

December 8, 2019

Why Crystal Calorimetry?

- Precision photons and electrons measurements enhance physics discovery potential in HEP experiments.
- Performance of crystal calorimeter is well understood for e/γ, and is investigated for jets measurements :
  - The best possible energy resolution and position resolution;
  - Good e/γ identification and reconstruction efficiency;
  - Excellent jet mass resolution with dual readout, either C/S and F/S gate.
- The next generation crystal detectors for HEP experiments:
  - Bright, fast and rad-hard LYSO and LuAG ceramics at the HL-LHC;
  - BaF_2:Y with <1 ns decay: ultrafast calorimetry for unprecedented rate;
  - Crystals with <$1/cc for the homogeneous hadron calorimetry.

Application of Ultrafast Crystals

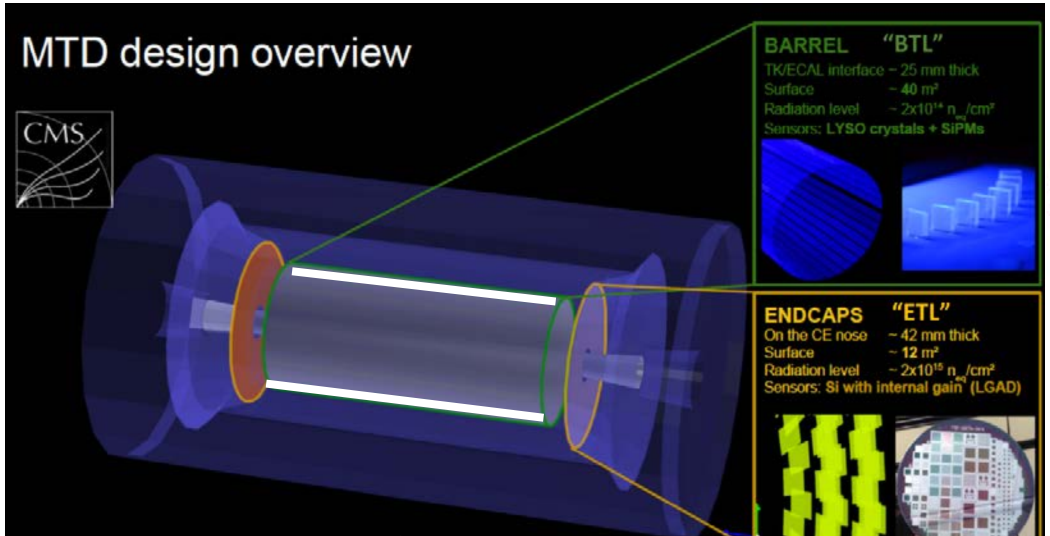

CMS BTL: An LYSO + SiPM Layer

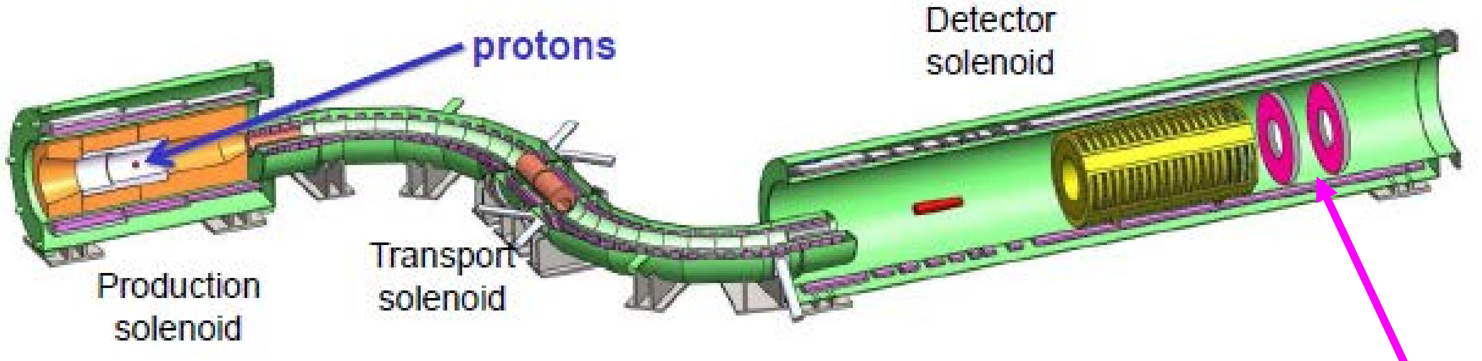

Mu2e-II: arXiv:1802.02599

Mu2e-I: 1,348 CsI of 34 x 34 x 200 mm

Mu2e-II: 1,940 BaF_2:Y of 30 x 30 x 218 mm

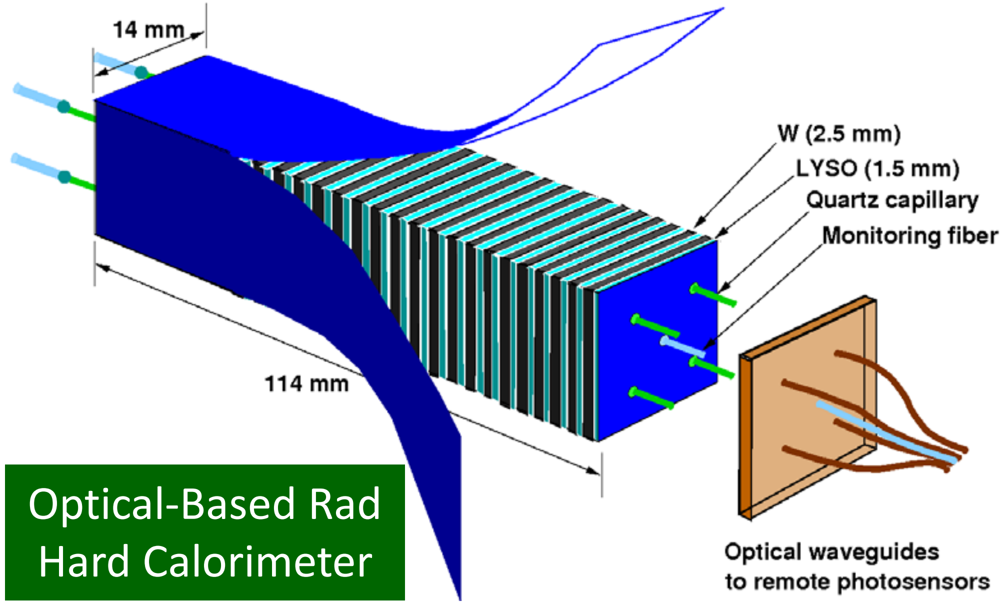

Optical-Based Rad Hard Calorimeter

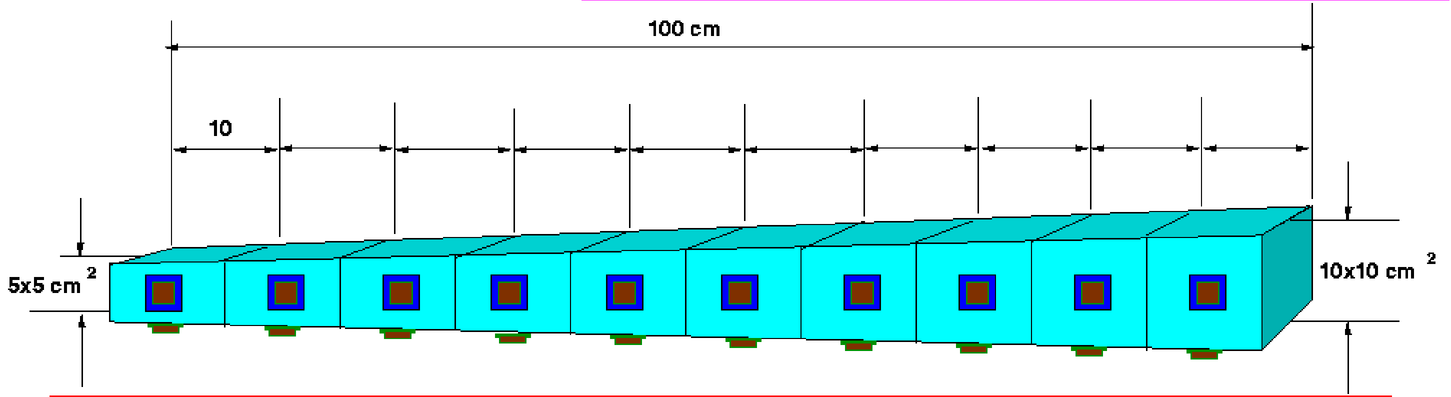

A. Para, H. Wenzel, and S. McGill, Callor2012 and A. Benaglia, E. Auffray, P. Lecoq, H. Wenzel, A. Para, IEEE Trans. Nucl. Sc. VOL. 13, NO. 9, Sept. 2014: GEANT simulations show a jet energy resolution at a level of 20%/√E by HHCAL with dual readout of S/C or gate.

Fast and Ultrafast Inorganic Scintillators

	BaF_2	BaF_2:Y	ZnO:Ga	YAP:Yb	YAG:Yb	β-Ga_2O_3	LYSO:Ce	LuAG:Ce	YAP:Ce	GAGG:Ce	LuYAP:Ce	YSO:Ce
Density (g/cm^3)	4.89	4.89	5.67	5.35	4.56	5.94[1]	7.4	6.76	5.35	6.5	7.2[f]	4.44
Melting points (^oC)	1280	1280	1975	1870	1940	1725	2050	2060	1870	1850	1930	2070
X_0 (cm)	2.03	2.03	2.51	2.77	3.53	2.51	1.14	1.45	2.77	1.63	1.37	3.10
R_M (cm)	3.1	3.1	2.28	2.4	2.76	2.20	2.07	2.15	2.4	2.20	2.01	2.93
λ_I (cm)	30.7	30.7	22.2	22.4	25.2	20.9	20.9	20.6	22.4	21.5	19.5	27.8
Z_{eff}	51.6	51.6	27.7	31.9	30	28.1	64.8	60.3	31.9	51.8	58.6	33.3
dE/dX (MeV/cm)	6.52	6.52	8.42	8.05	7.01	8.82	9.55	9.22	8.05	8.96	9.82	6.57
λ_{peak}[a] (nm)	300 220	300 220	380	350	350	380	420	520	370	540	385	420
Refractive Index[b]	1.50	1.50	2.1	1.96	1.87	1.97	1.82	1.84	1.96	1.92	1.94	1.78
Normalized Light Yield[a,c]	42 4.8	1.7 4.8	6.6[d]	0.19[d]	0.36[d]	6.5 0.5	100	35[e] 48[e]	9 32	115	16 15	80
Total Light yield (ph/MeV)	13,000	2,000	2,000[d]	57[d]	110[d]	2,100	30,000	25,000[e]	12,000	34,400	10,000	24,000
Decay time[a] (ns)	600 <0.6	600 <0.6	<1	1.5	4	148 6	40	820 50	191 25	800 80	1485 36	75
LY in 1[st] ns (photons/MeV)	1200	1200	610[d]	28[d]	24[d]	43	740	240	391	640	125	318
40 keV Att. Leng. (1/e, mm)	0.106	0.106	0.407	0.314	0.439	0.394	0.185	0.251	0.314	0.319	0.214	0.334

Expected Radiation at the HL-LHC

CMS MTD: 4.8 Mrad, 2.5x 10^{13} p/cm^2 & 3.2 x 10^{14} n_{eq}/cm^2
CMS FCAL: 68 Mrad, 2.1x 10^{14} p/cm^2 & 2.4 x 10^{15} n_{eq}/cm^2

CMS MTD	η	n_{eq} (cm^{-2})	n_{eq} Flux (cm^{-2}s^{-1})	Protons (cm^{-2})	p Flux (cm^{-2}s^{-1})	Dose (Mrad)	Dose rate (rad/h)
Barrel	0.00	2.48E+14	2.75E+06	2.2E+13	2.4E+05	2.7	108
Barrel	1.15	2.70E+14	3.00E+06	2.4E+13	2.6E+05	3.8	150
Barrel	**1.45**	**2.85E+14**	**3.17E+06**	**2.5E+13**	**2.8E+05**	**4.8**	**192**
Endcap	1.60	2.3E+14	2.50E+06	2.0E+13	2.2E+05	2.9	114
Endcap	2.00	4.5E+14	5.00E+06	3.9E+13	4.4E+05	7.5	300
Endcap	2.50	1.1E+15	1.25E+07	9.9E+13	1.1E+06	25.5	1020
Endcap	**3.00**	**2.4E+15**	**2.67E+07**	**2.1E+14**	**2.3E+06**	**67.5**	**2700**

Particle Energy Spectra at the HL-LHC

FLUKA simulations: neutrons and charged hadrons peaked at MeV and several hundreds MeV, respectively. Neutron and proton induced damages were investigated at the East Port and the Blue Room of the Los Alamos Neutron Science Center (LANSCE), respectively

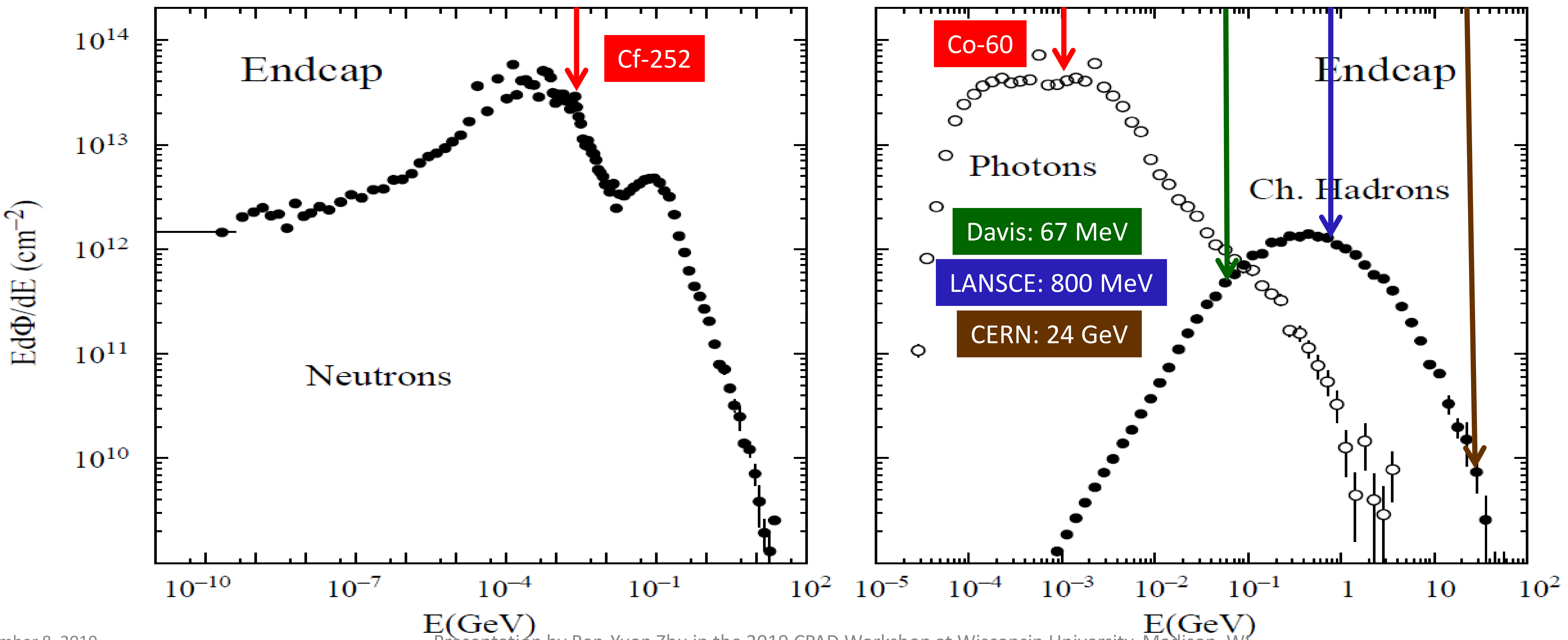

QC on Radiation Induced Readout Noise

Radiation induced readout noise (~30 keV) was determined by measuring the radiation induced photo-current in LYSO+SiPM under the expected dose rate and neutron fluence

$$F = \frac{\dfrac{Photocurrent}{Charge_{electron} \times Gain_{SiPM}}}{Dose\ rate_{\gamma-ray}\ or\ Flux_{neutron}} \qquad \sigma = \frac{\sqrt{Q}}{LO}\ \text{(MeV)}$$

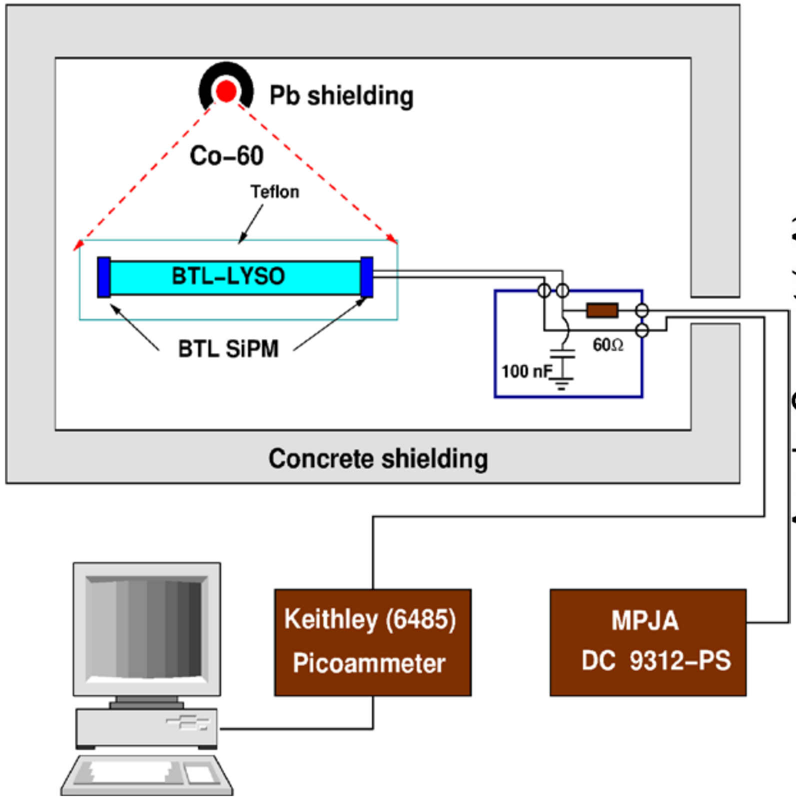

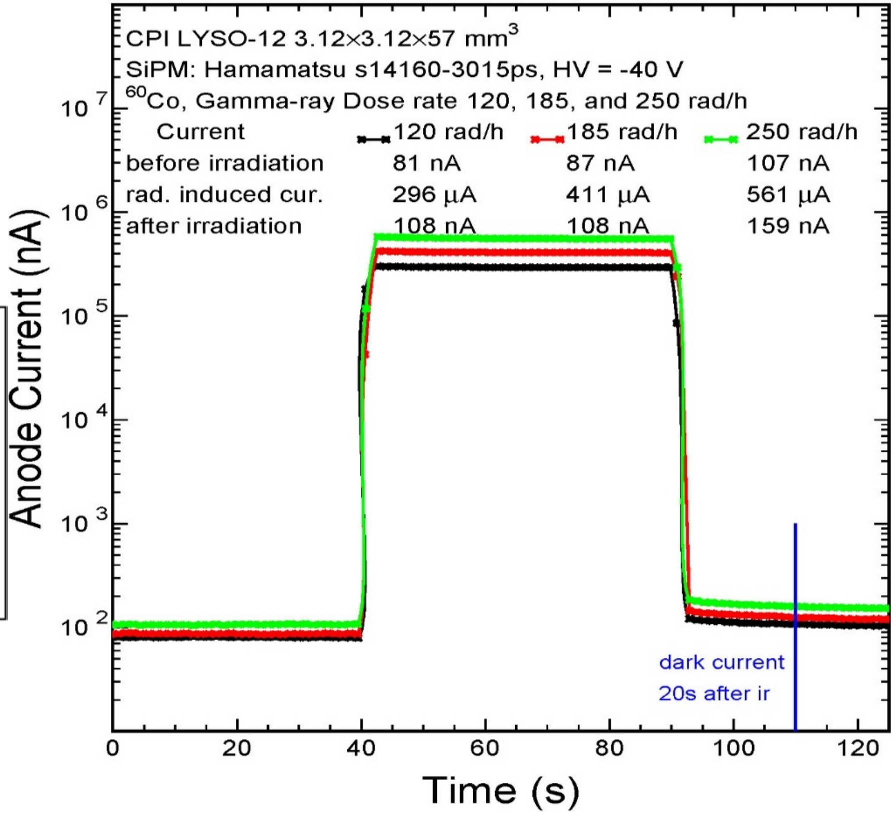

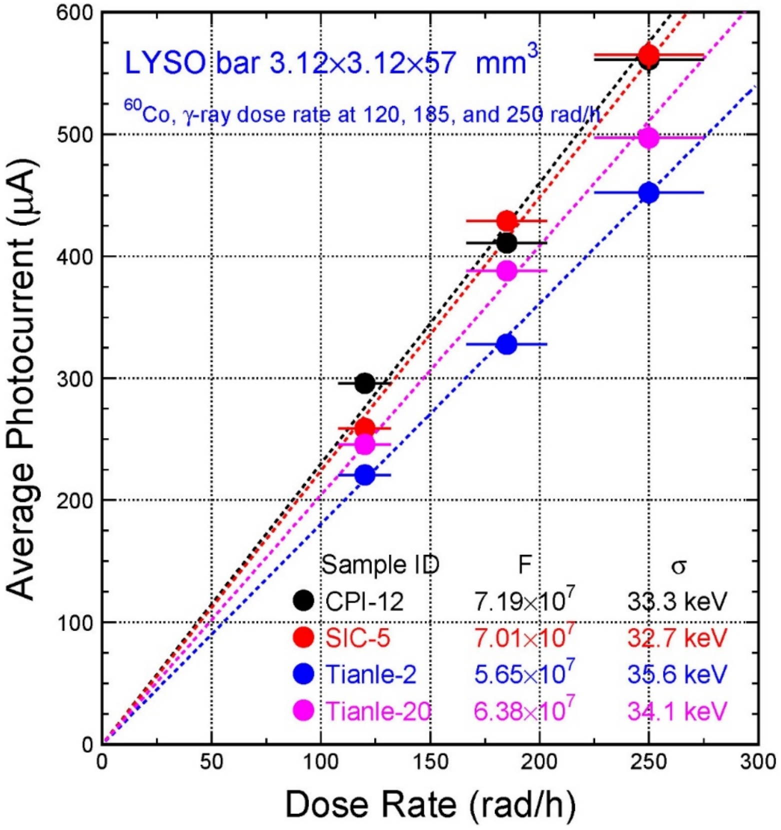

Total Hadron Fluence at LANSCE

Irradiation by 800 MeV protons in three experiments 6501, 6990 and 7324 up to 3 x 10^{15} p/cm^2 was carried out in the blue room of LANSCE, where crystals and shashlik calorimeter towers were measured *in situ* by a home-made spectrophotometer.

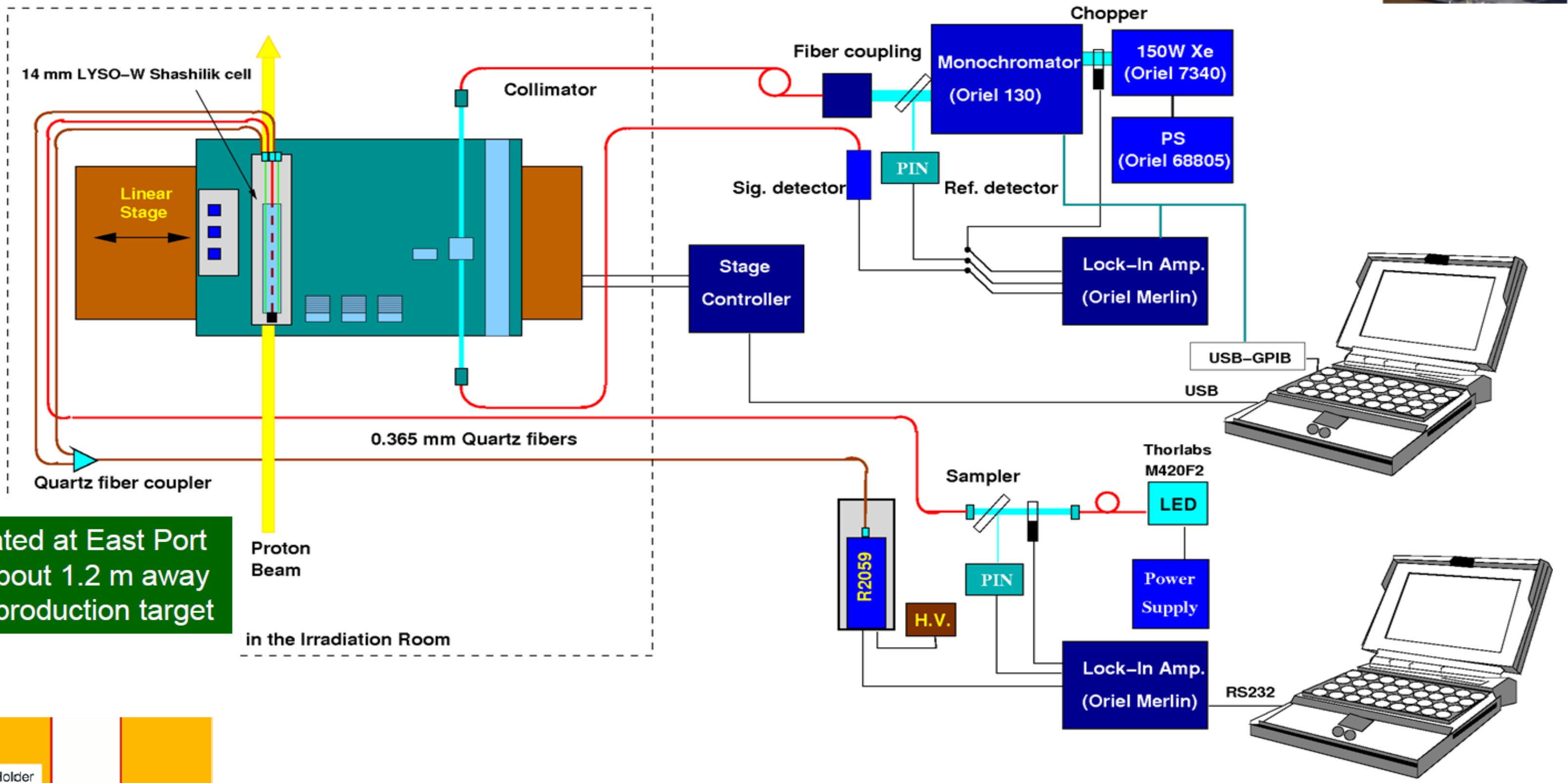

Los Alamos Neutron Science Center (LANSCE)

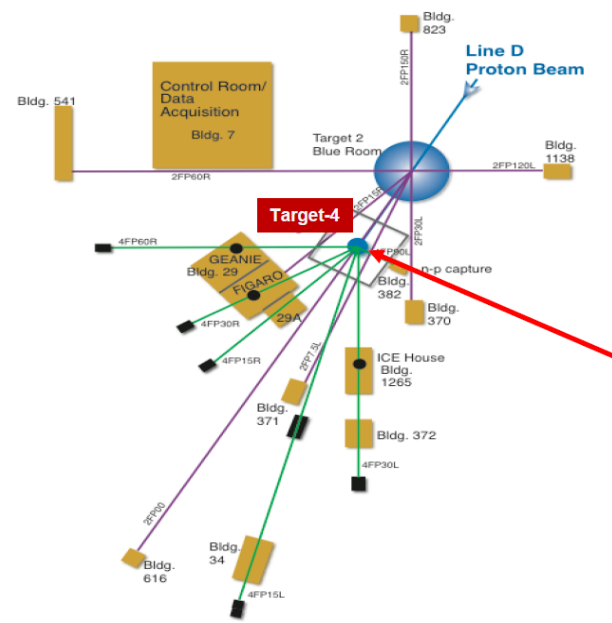

Samples are located at East Port in the Target-4, about 1.2 m away from the neutron production target

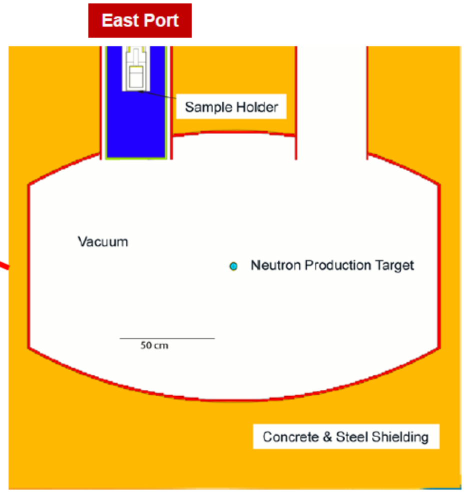

Irradiation by neutrons in three experiments 6991, 7332 and 7638 up to 3 x 10^{15} n_{eq}/cm^2 in the East Port of LANSCE with 1 MeV equivalent neutron flux calculated by using MCNPX (Monte Carlo N-Particle eXtended) package tallied in the largest sample volume (averaging).

LYSO Radiation Hardness

CMS BTL radiation spec: < 3 m^{-1} after 4.8 Mrad, 2.5 x 10^{13} p/cm^2 and 3.2 x 10^{14} n_{eq}/cm^2

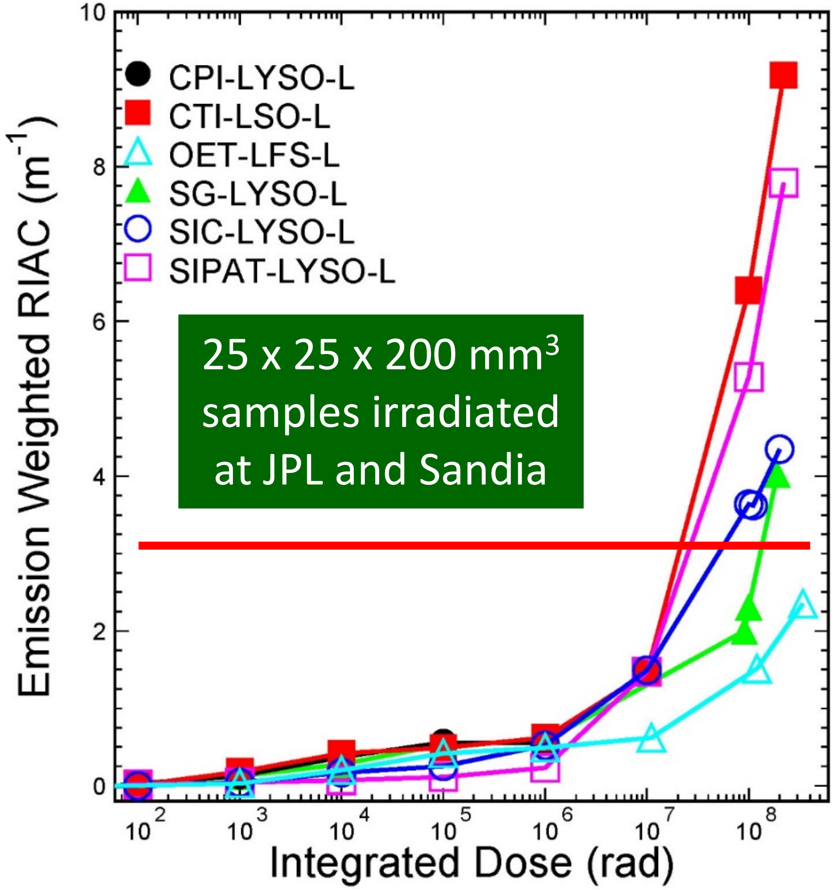

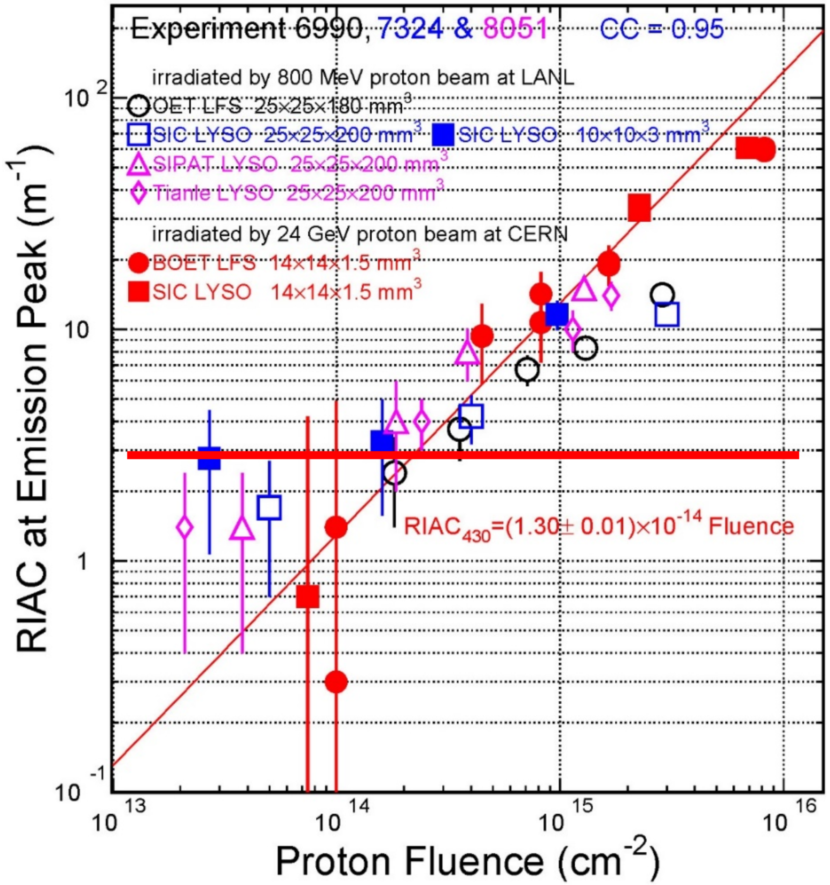

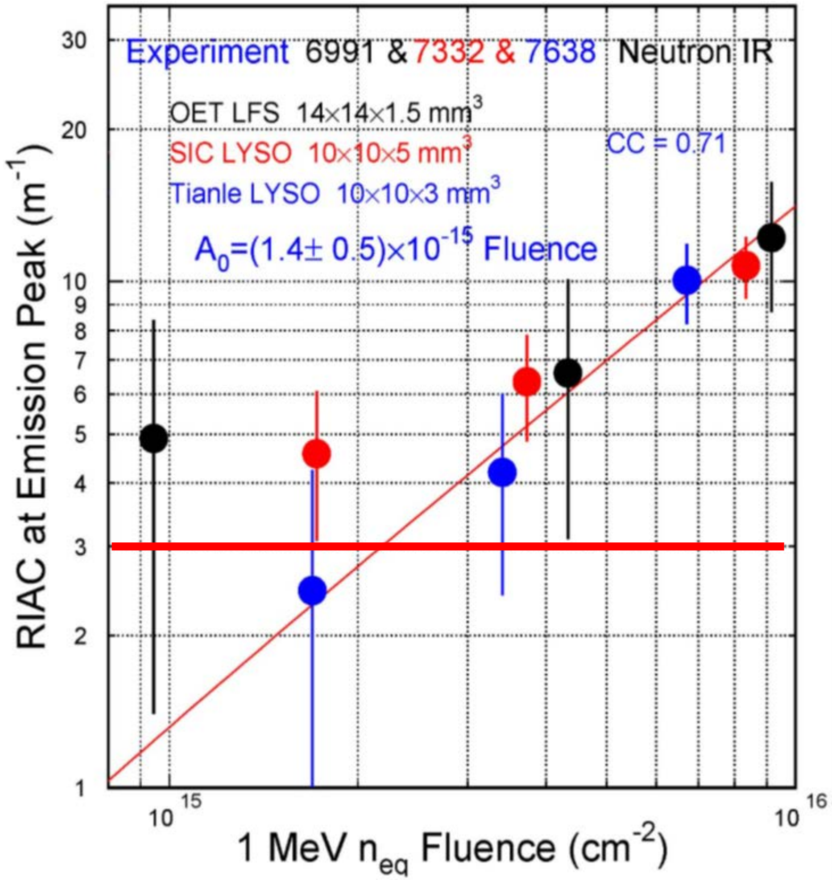

Damage induced by protons is an order of magnitude larger than that from neutrons due to ionization energy loss in addition to displacement and nuclear breakup

LuAG:Ce Ceramic Samples

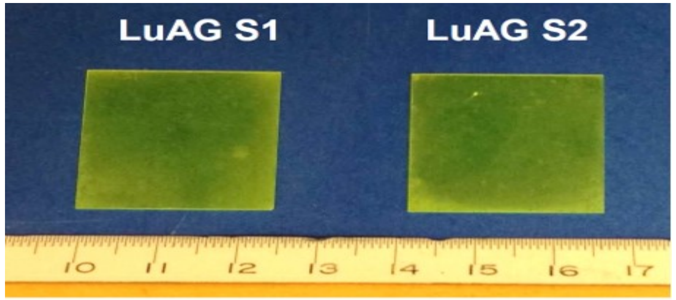

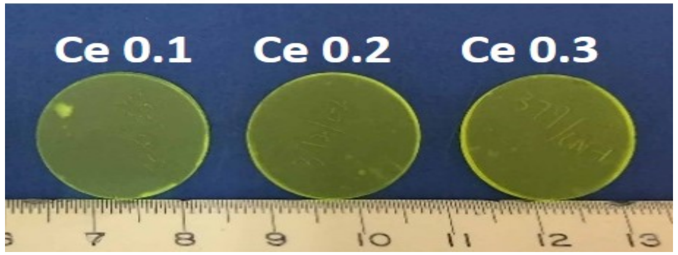

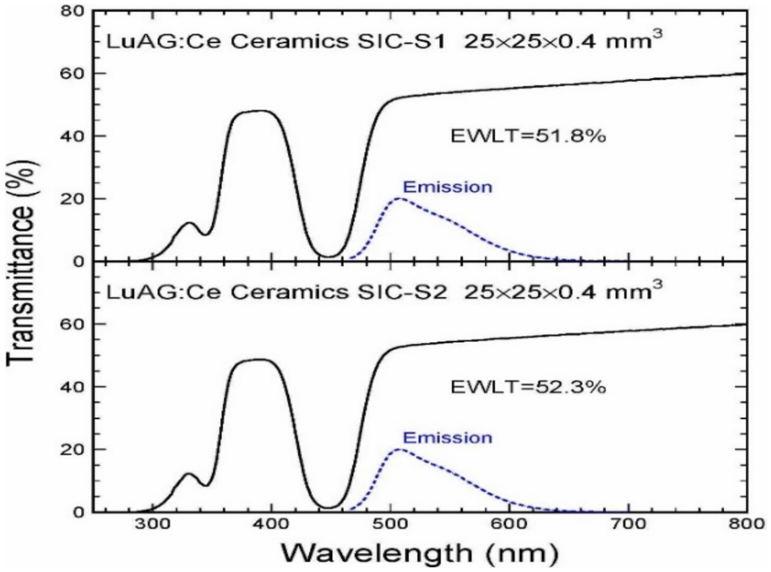

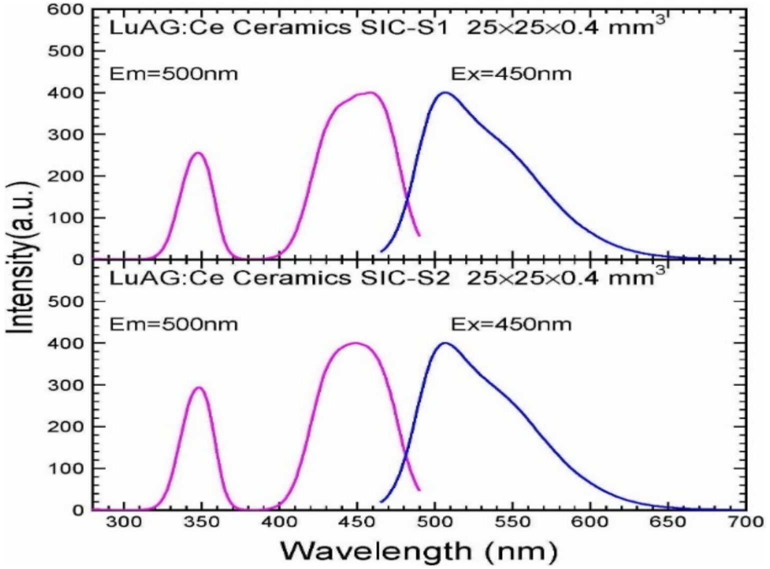

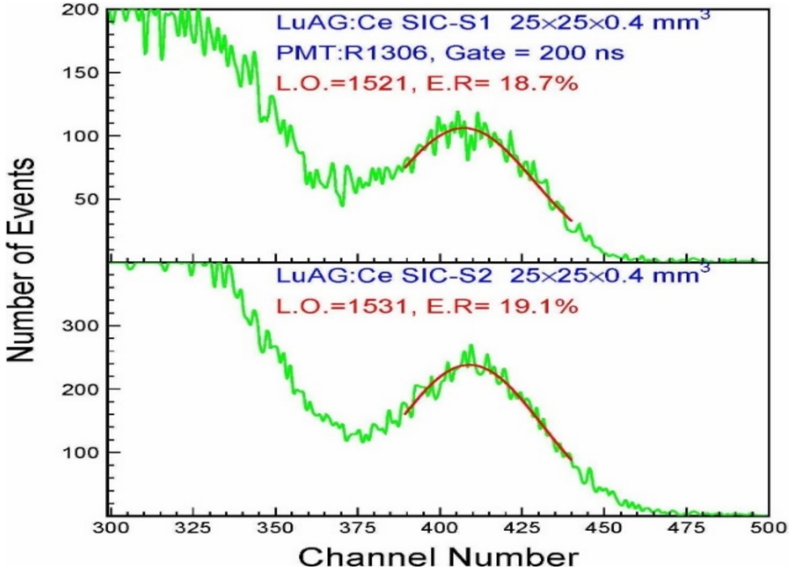

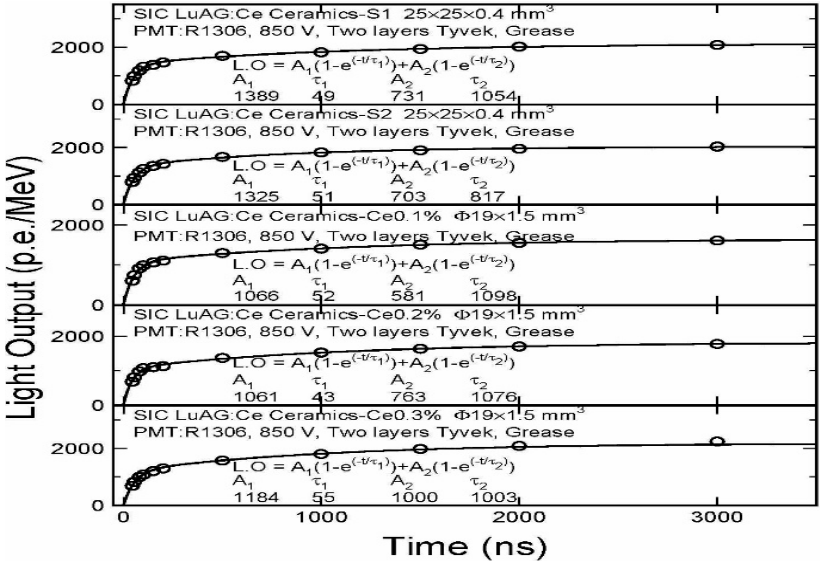

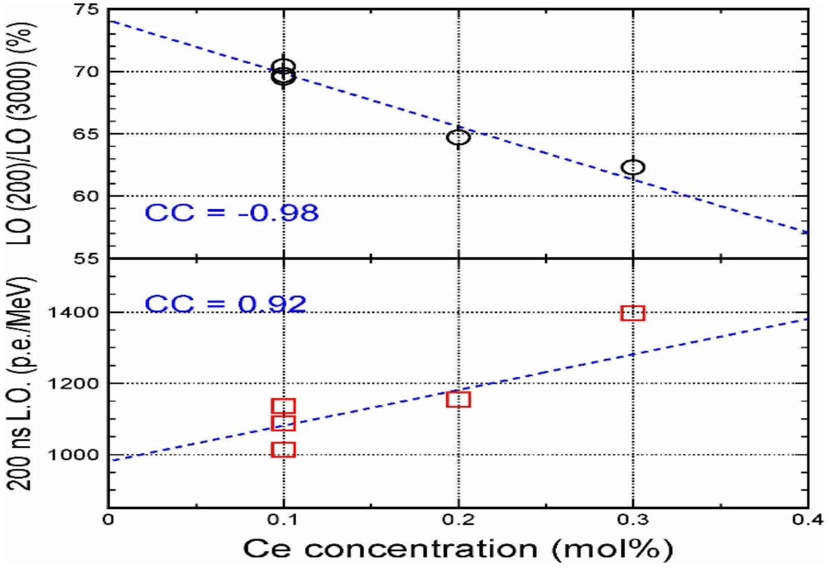

Radiation Hard LuAG:Ce Ceramics

Investigated at LANSCE up to 3×10^{14} p/cm^2 of 800 MeV, and at Sadia up to 220 Mrad

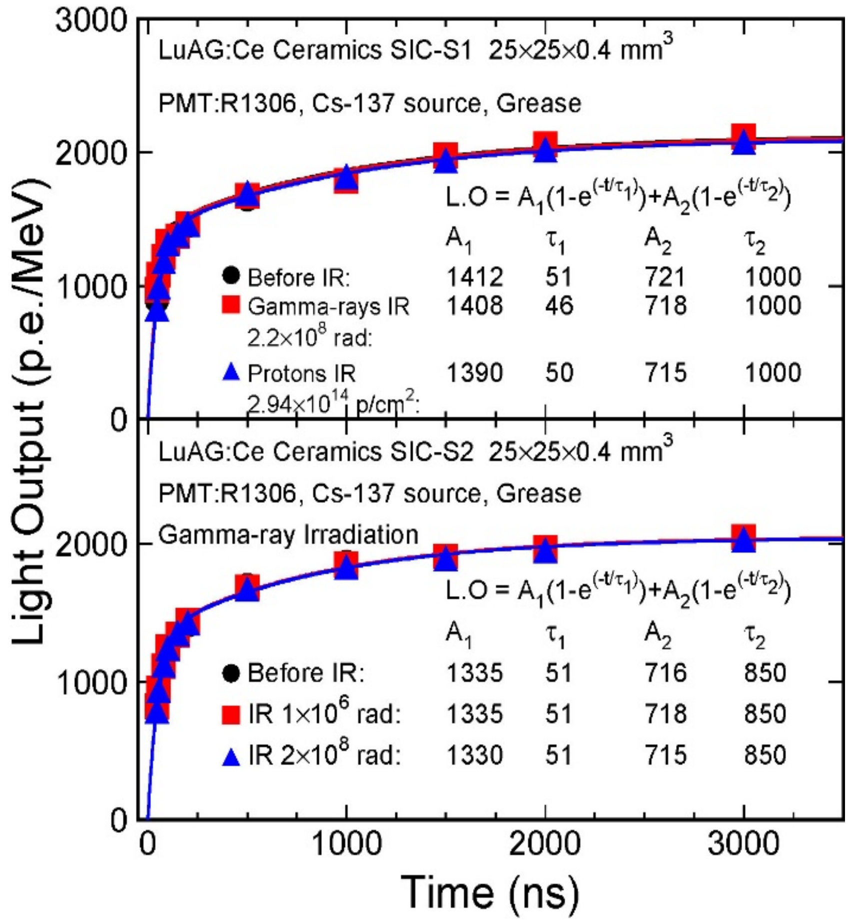

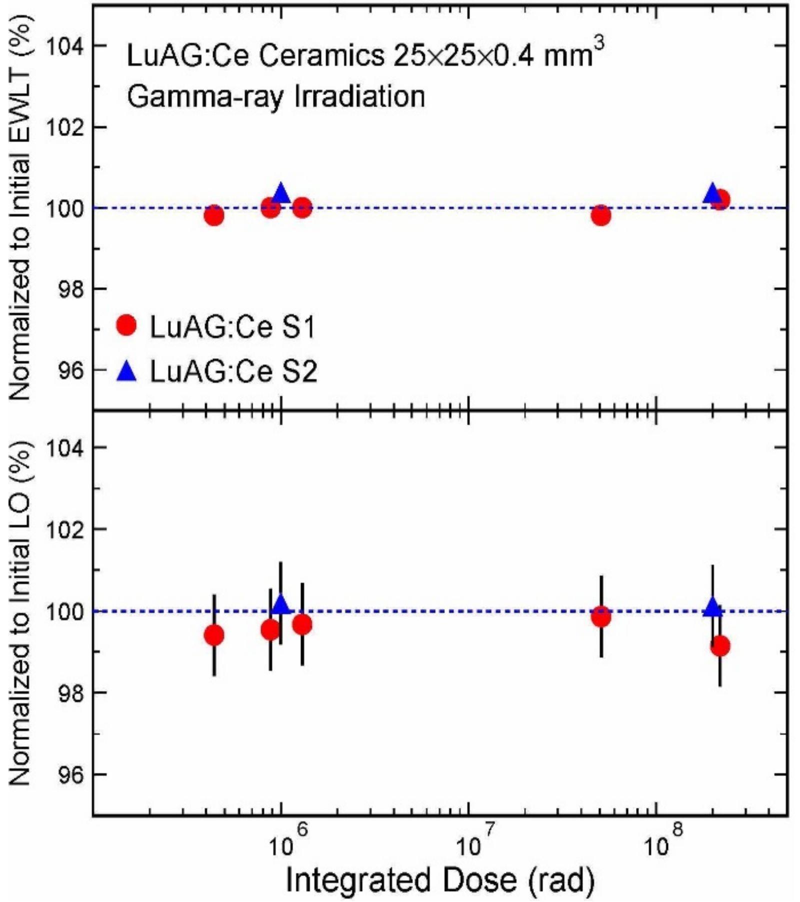

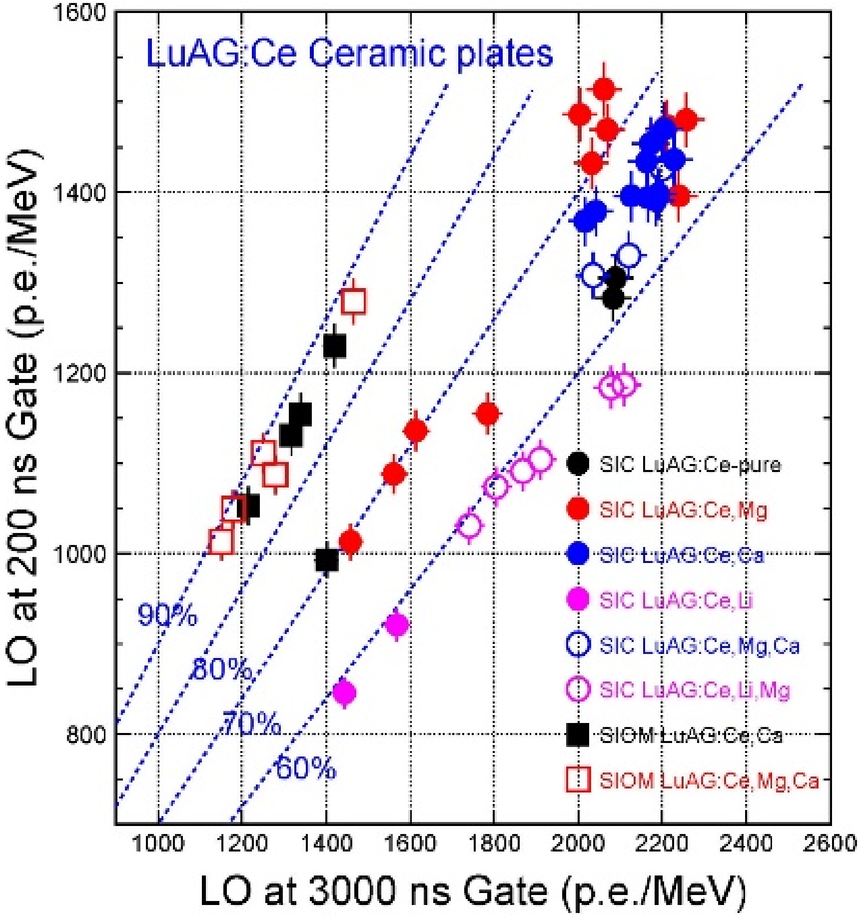

R&D on-going to suppress μs slow component by Pr doping or co-doping

γ-Ray Induced Damage in Large BaF_2

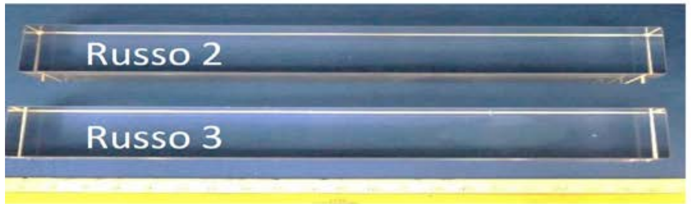

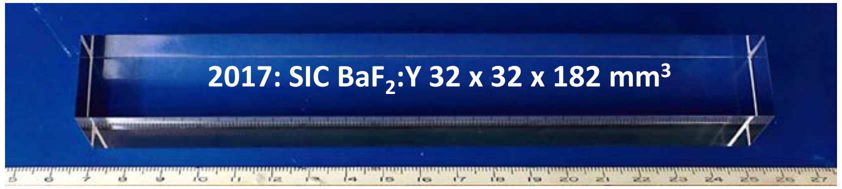

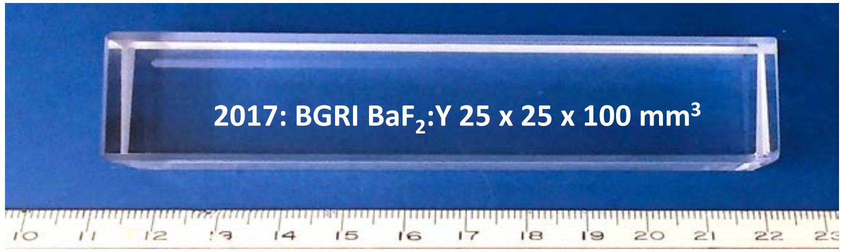

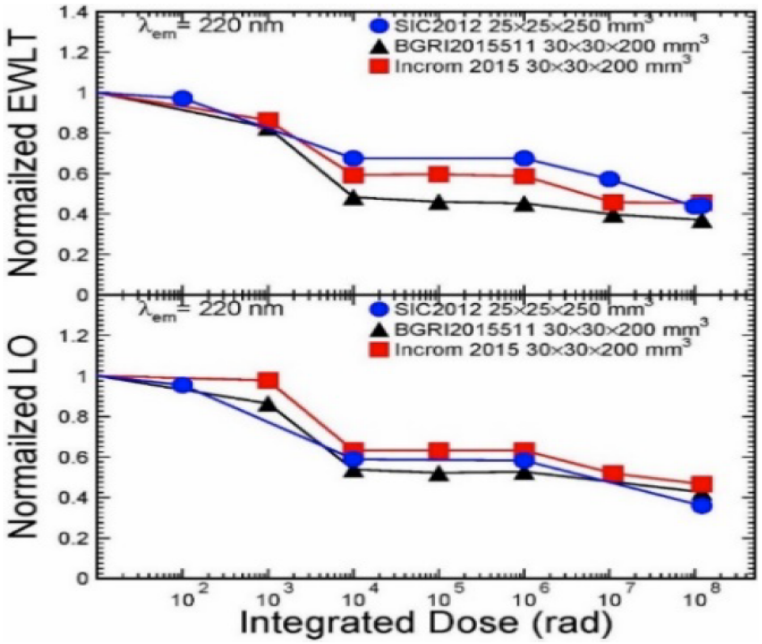

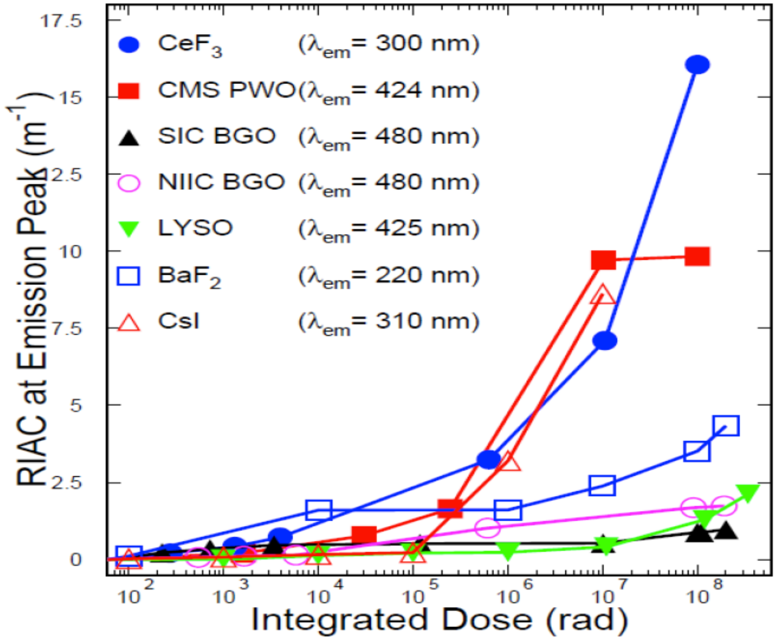

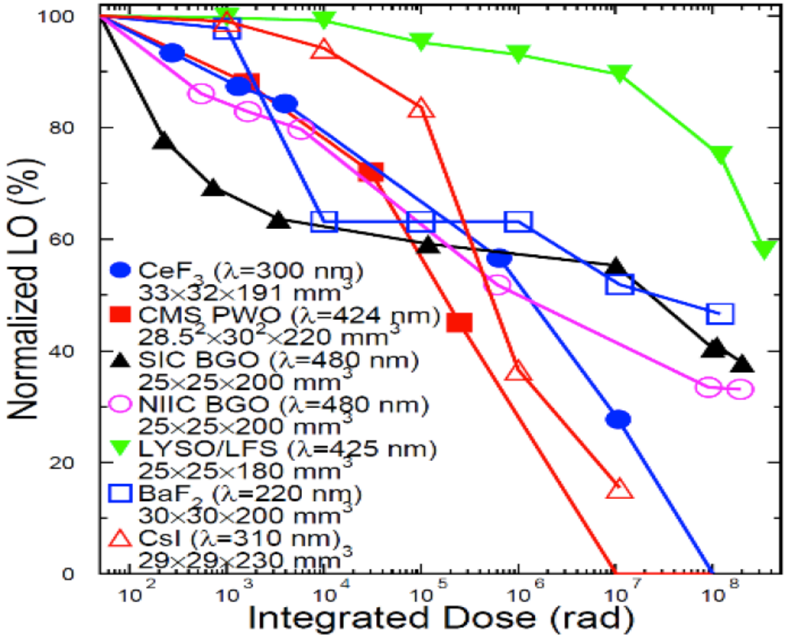

Proton and Neutron Induced Damage in BaF_2

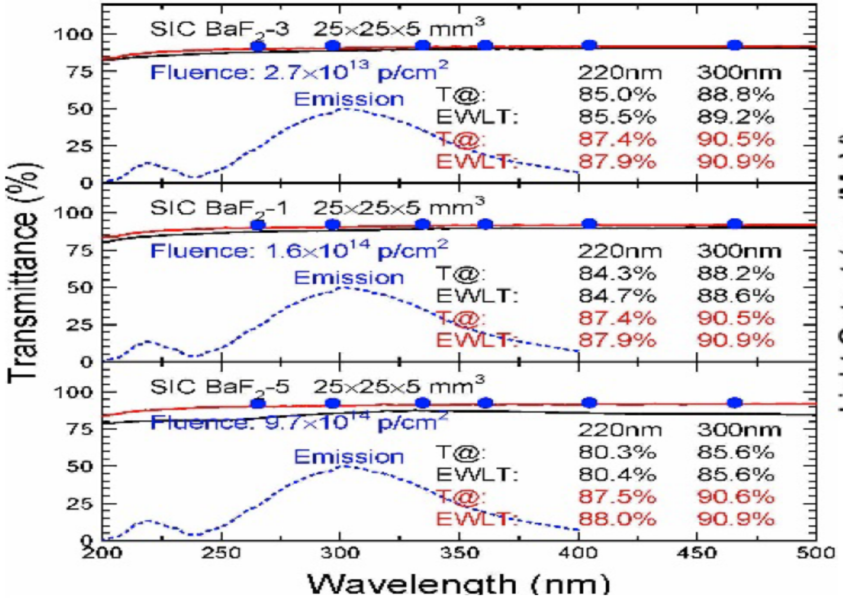

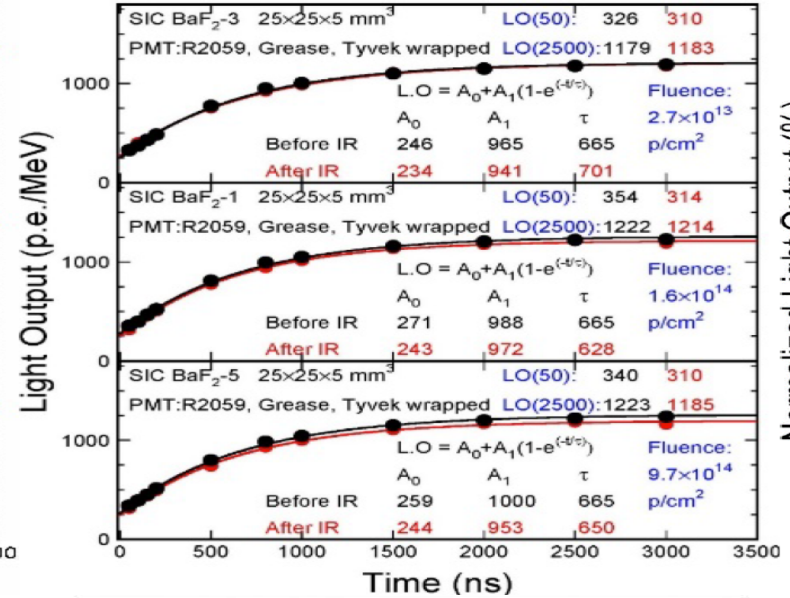

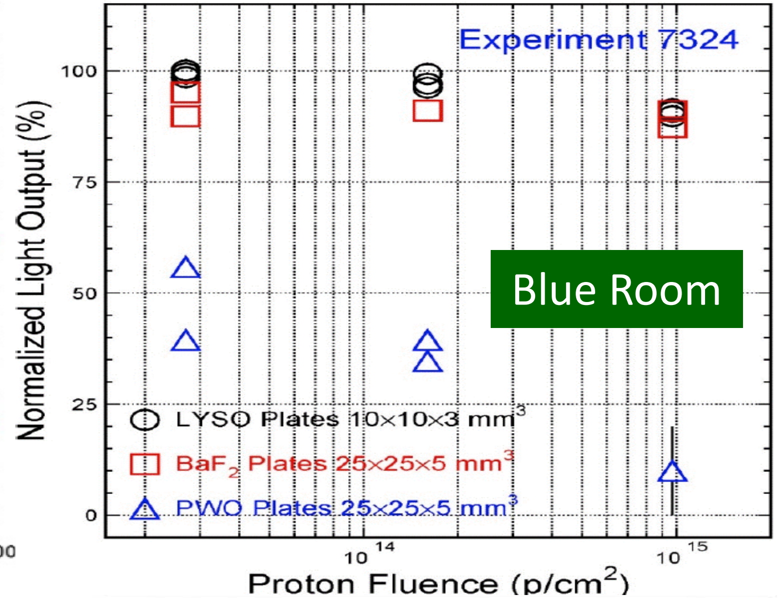

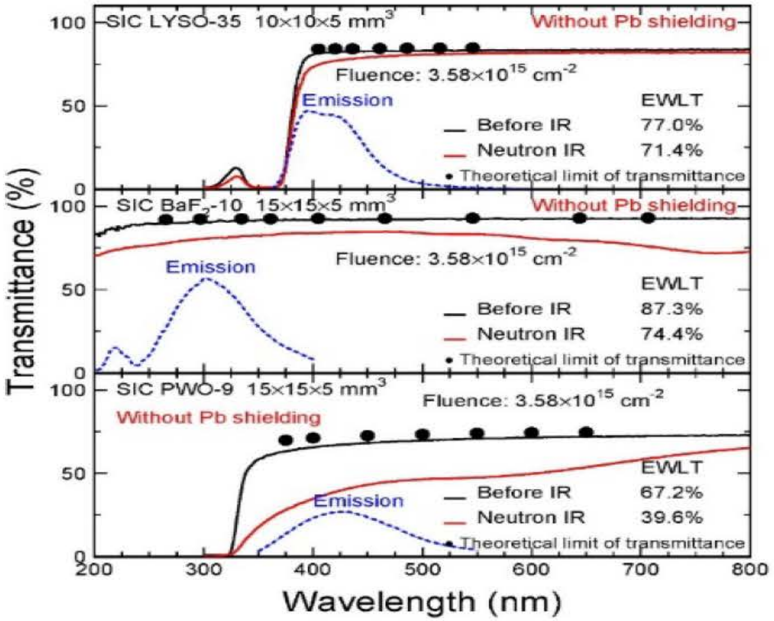

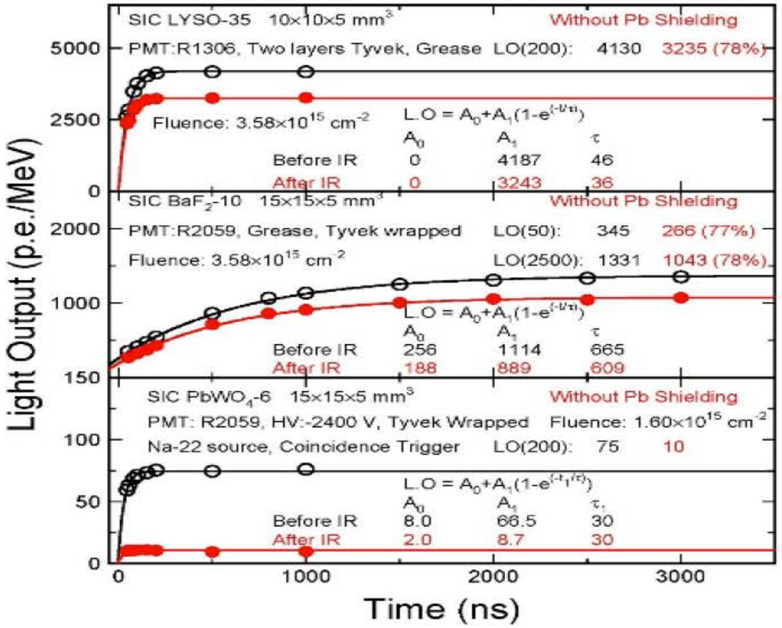

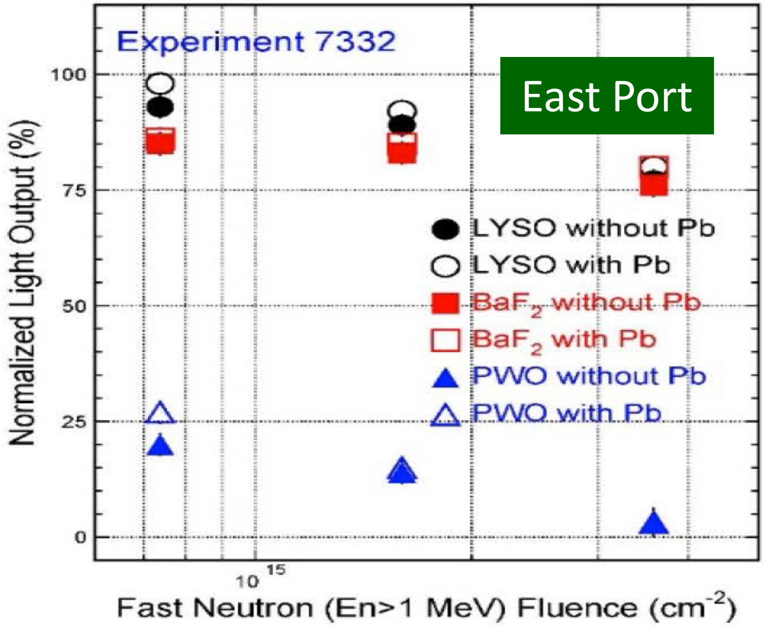

Ultrafast and Slow Light from BaF_2

BaF_2 has an ultrafast scintillation component with sub-ns decay, and a 600 ns slow component.

The amount of the fast light is similar to undoped CsI, and is 1/5 of the slow component.

Selective readout of the ultrafast component may be realized by (1) selective doping in crystals or (2) selective readout with solar blind photodetector.

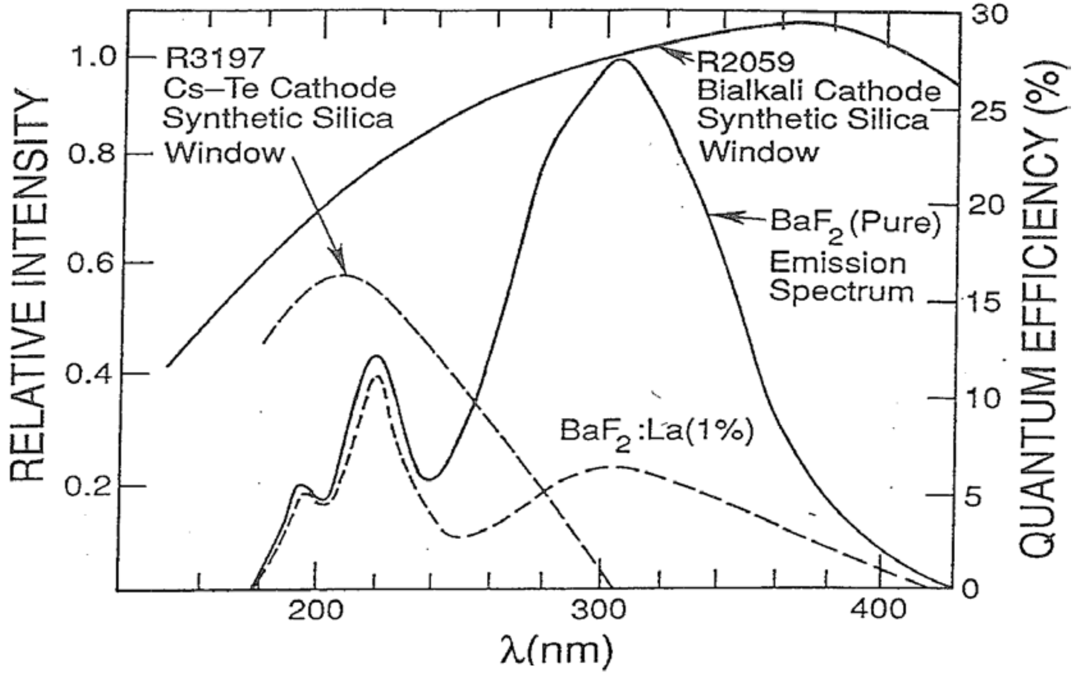

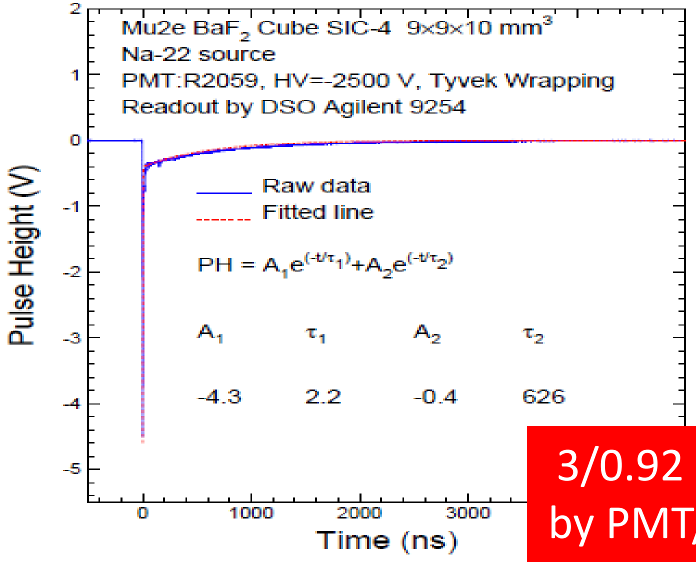

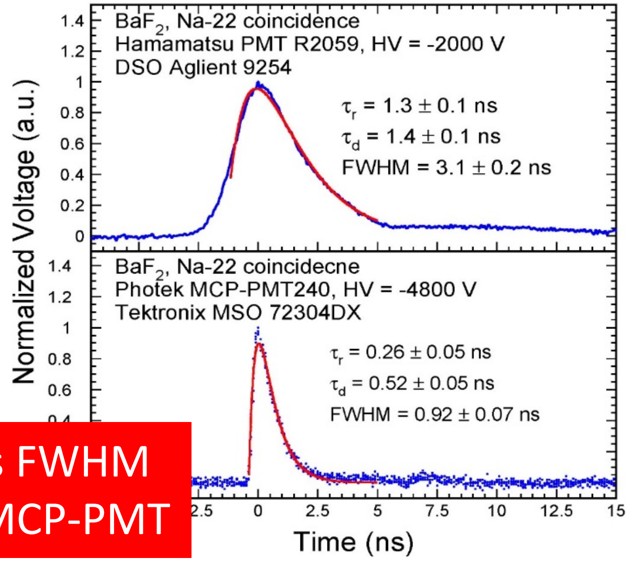

3/0.92 ns FWHM by PMT/MCP-PMT

Yttrium Doped Barium Fluoride: BaF_2:Y

Significant increased F/S ratio in BaF_2:Y; Sub-ns FWHM by MCP-PMT

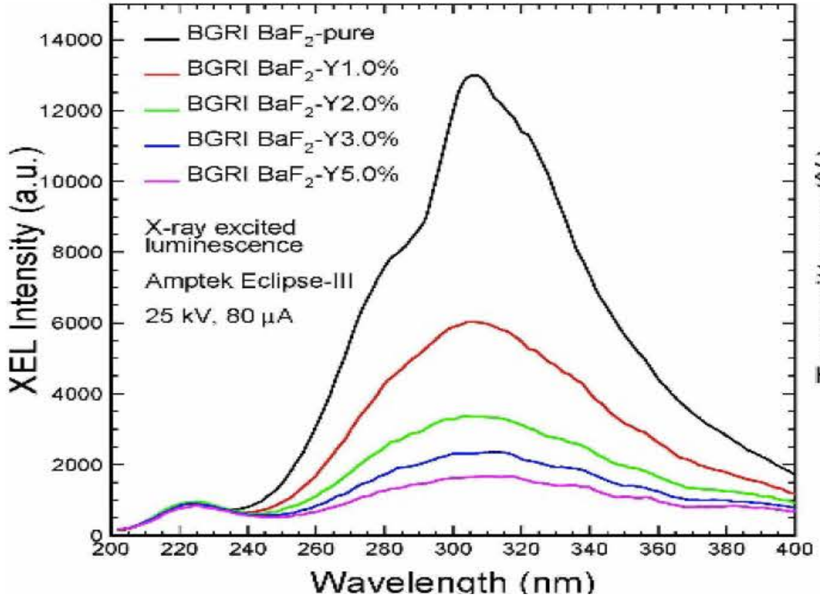

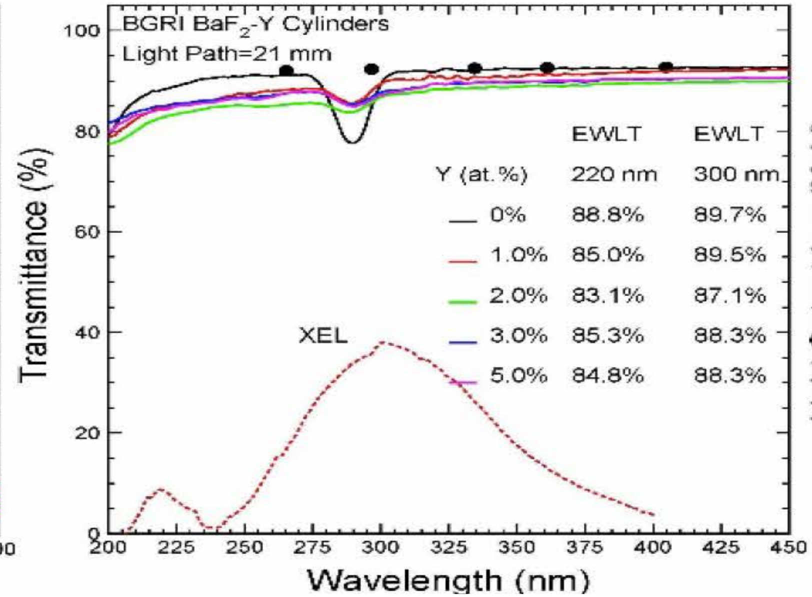

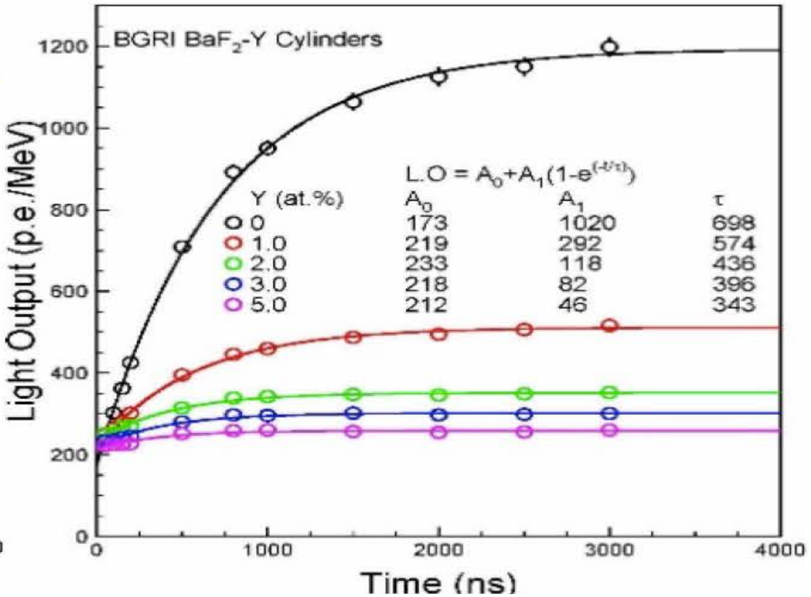

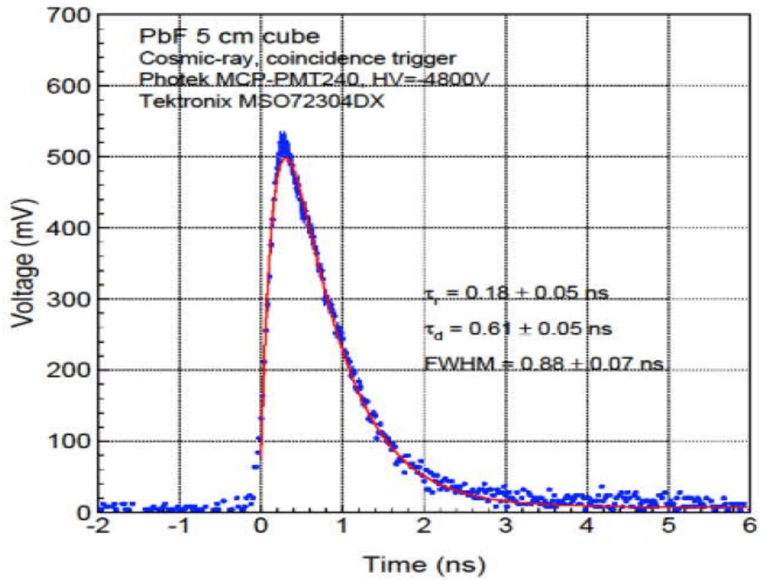

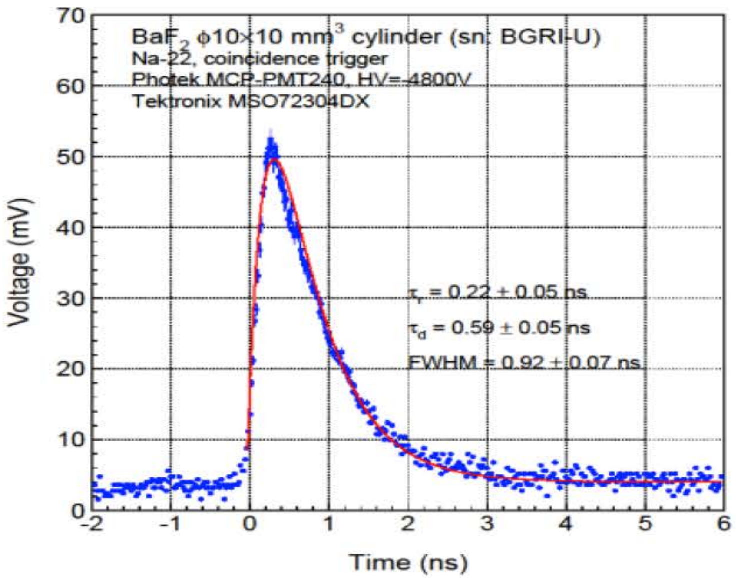

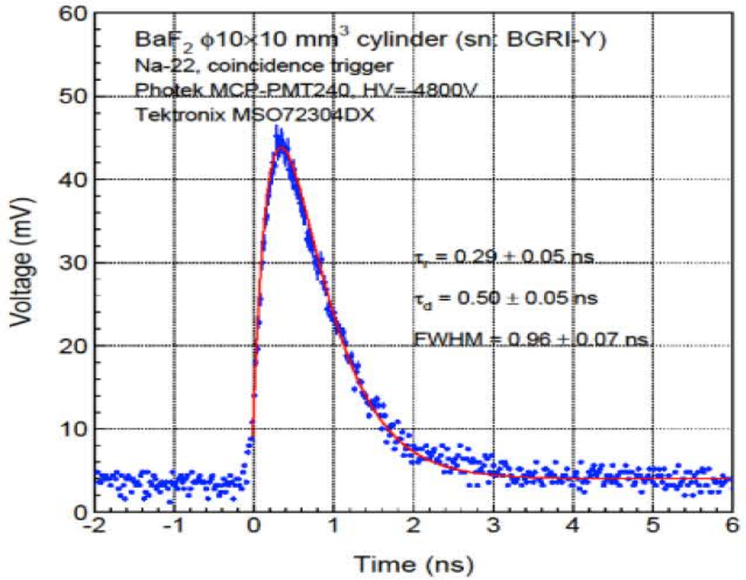

APS Beam Test: Other Fast Crystals

YAP:Yb, ZnO:Ga, YAG:Yb and GaO have pulse width less than 10 ns

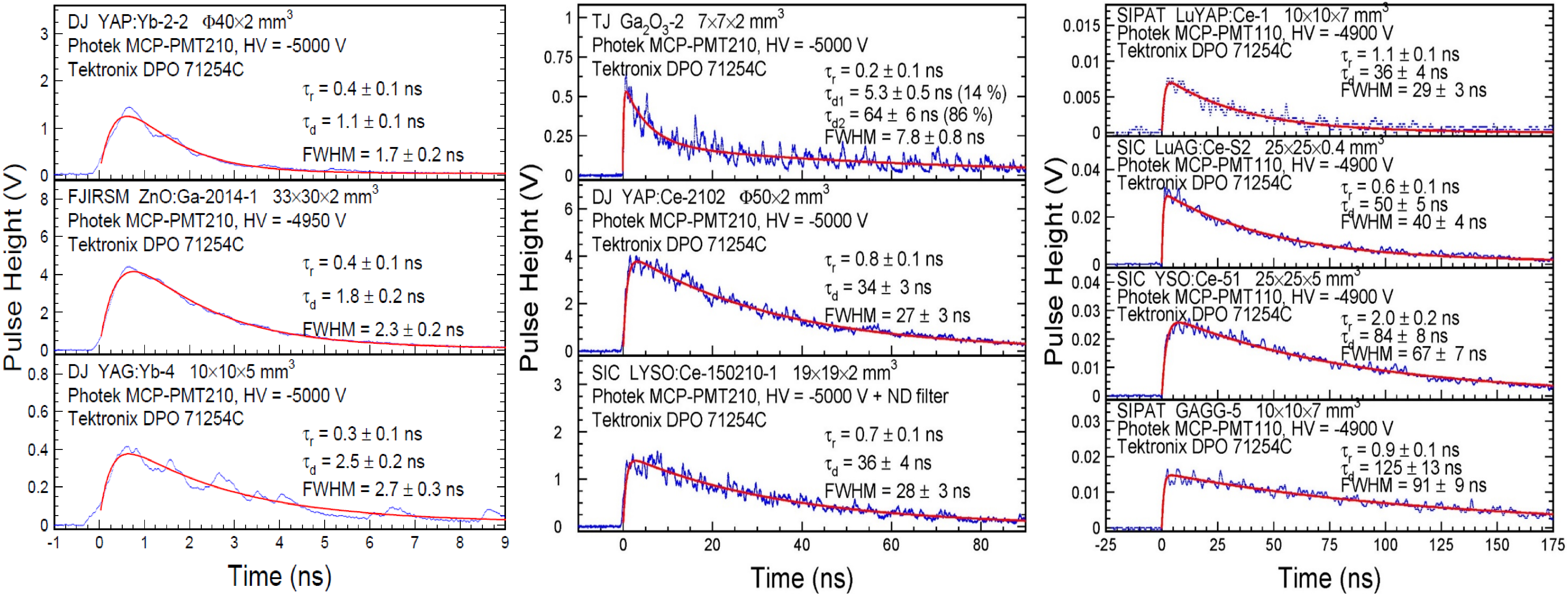

Decay time consists with our Lab data measured with γ-ray source

APS Beam Test: BaF_2:Y, BaF_2, ZnO:Ga & LYSO

X-ray bunches with 2.83 ns spacing in septuplet are clearly resolved by ultrafast BaF_2:Y and BaF_2 crystals, showing a proof-of-principle for the type –I imager

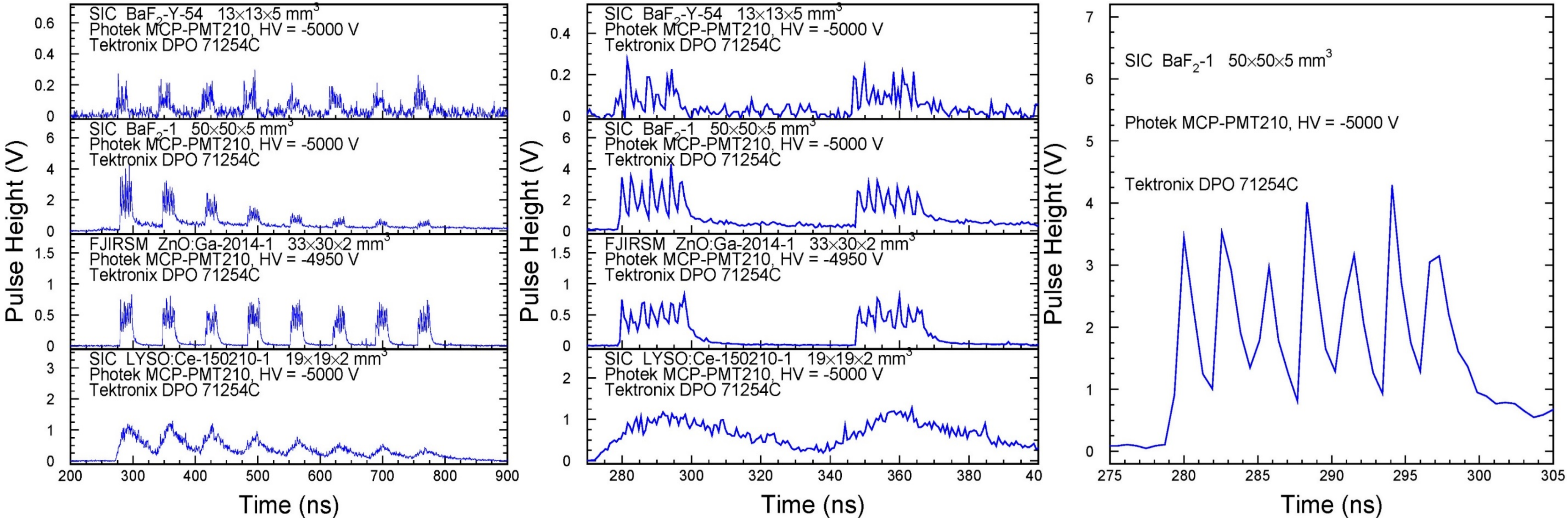

Amplitude reduction in BaF_2 and LYSO due to space charge in PMT from slow scintillation, but not in BaF_2:Y

Progress in Large Size BaF_2:Y Crystals

Two large size BaF_2:Y samples grown at SIC and BGRI in 2019
Improved optical quality, F/S ratio and light response uniformity

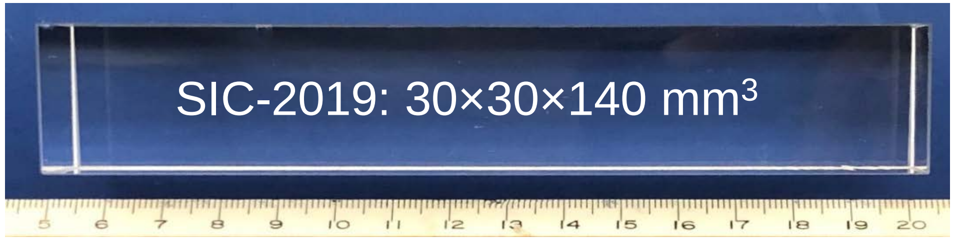

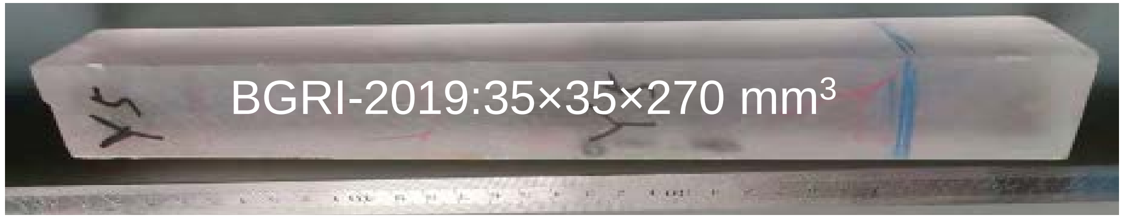

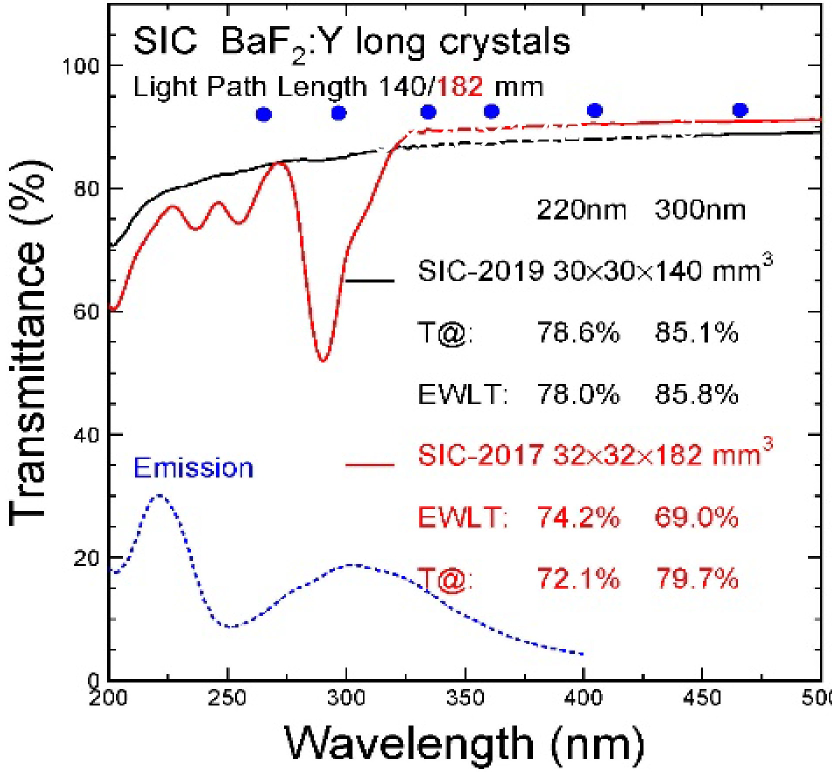

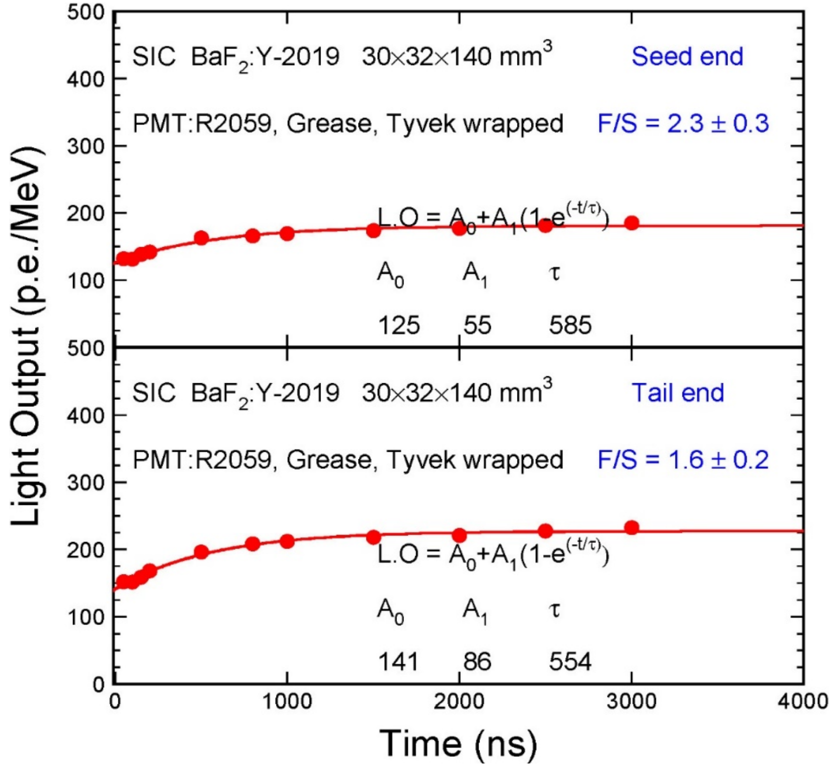

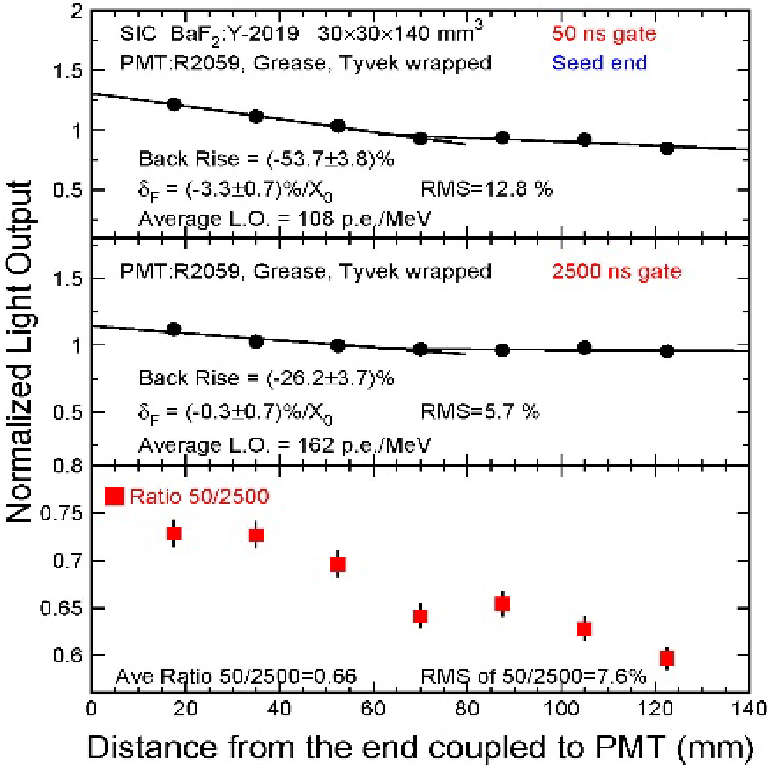

UV Photo-Detector for BaF_2 and BaF_2:Y

Photo-detectors	EWQE$_{fast}$ (%)	EWQE$_{slow}$ (%)	BaF_2 LO$_{fast}$	BaF_2 LO$_{slow}$	BaF_2 F/S	BaF_2:Y LO$_{fast}$	BaF_2:Y LO$_{slow}$	BaF_2:Y F/S
Hamamatsu R2059	15.2	20.9	0.15	1.07	1/7.0	0.15	0.32	1/2.1
Photek solar blind PMT	25.6	10.6	0.26	0.54	1/2.1	0.25	0.15	1/0.6
Hamamatsu s1337x	21.7	18.2	0.22	0.93	1/4.3	0.22	0.28	1/1.3

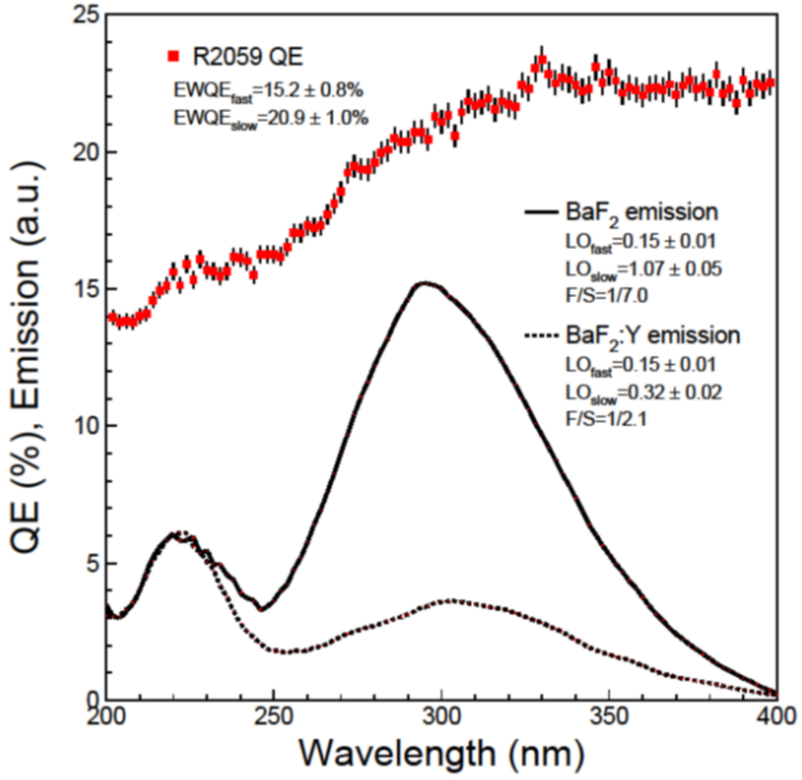

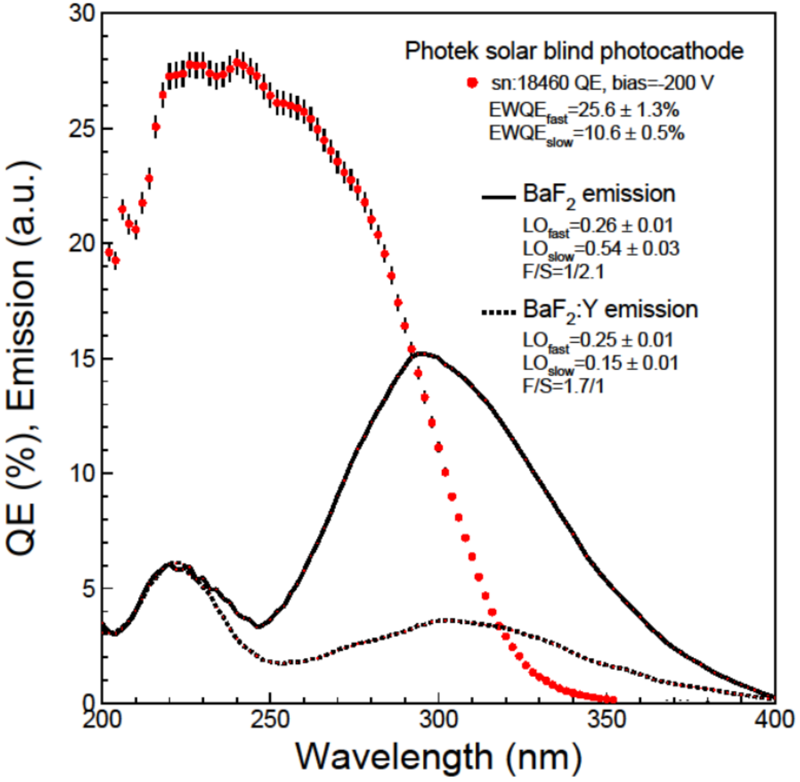

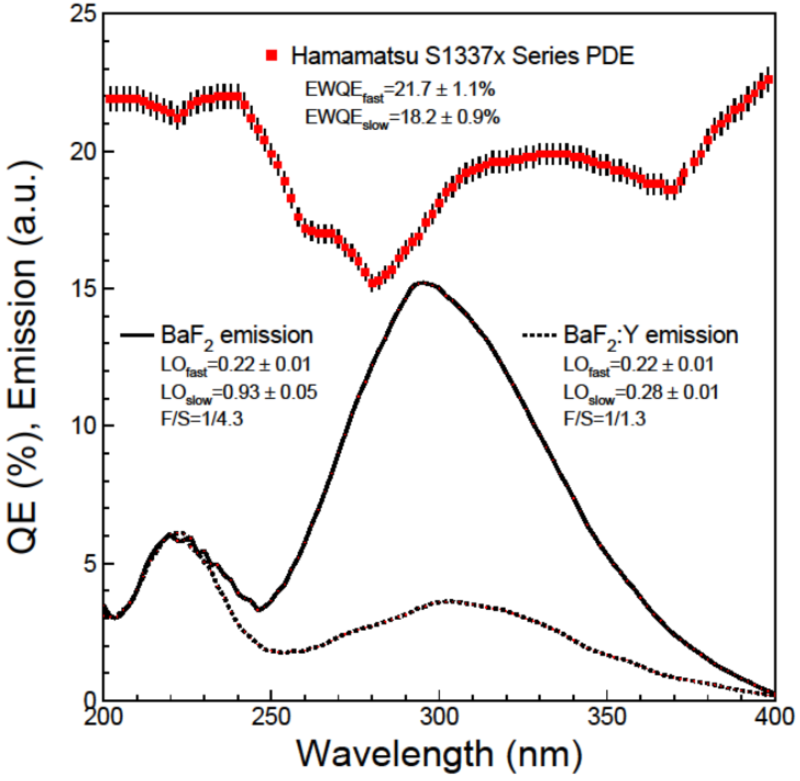

HHCAL Detector Concept

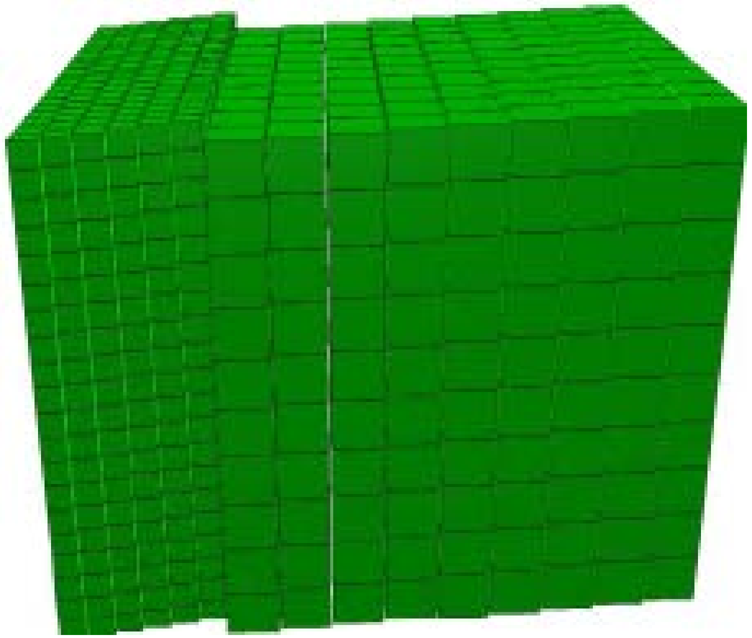

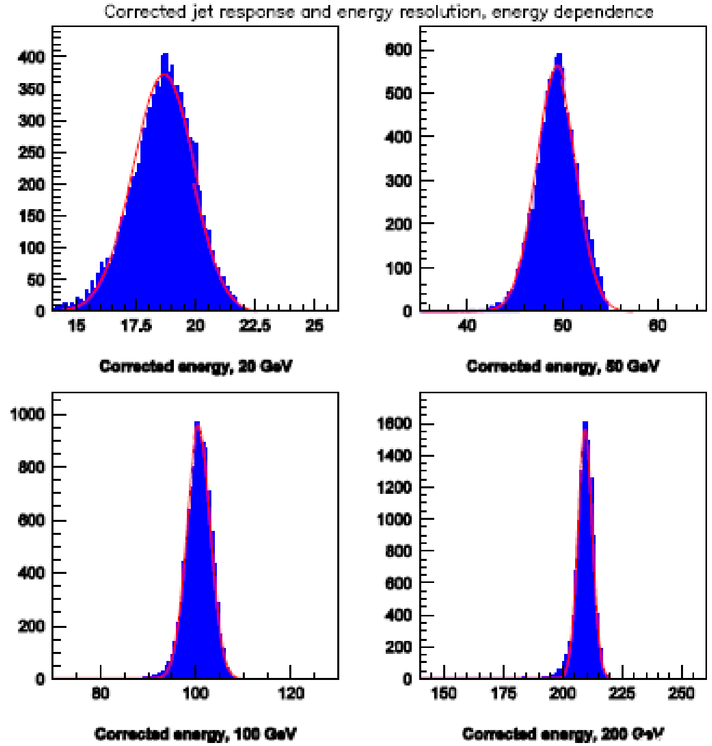

A. Para, H. Wenzel, and S. McGill, Callor2012: GEANT simulations show a jet energy resolution at a level of 20%/√E.
A. Benaglia, E. Auffray, P. Lecoq, H. Wenzel, A. Para, IEEE Trans. Nucl. Sc. VOL. 13, NO. 9, Sept. 2014, shows similar resolution can be achieved with dual gate.

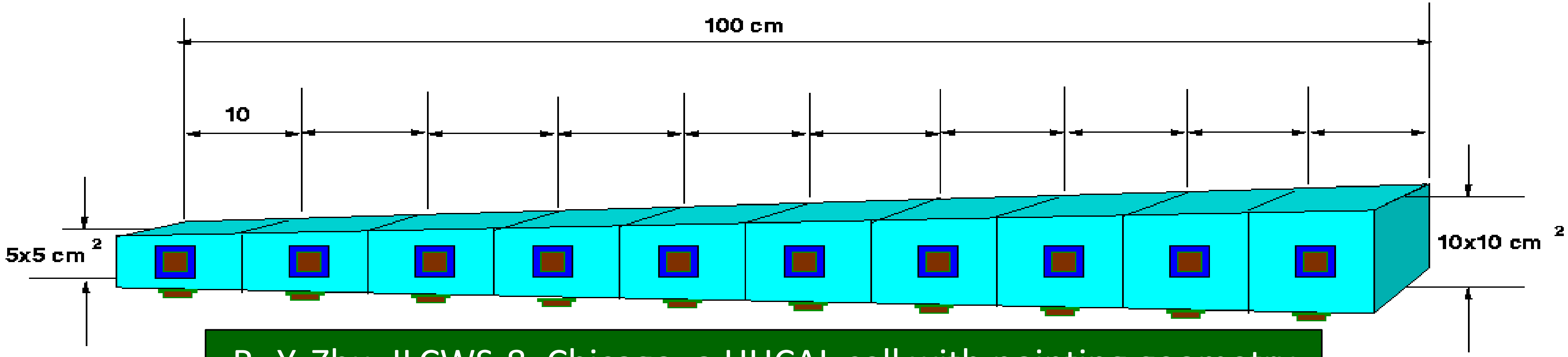

R.-Y. Zhu, ILCWS-8, Chicago: a HHCAL cell with pointing geometry

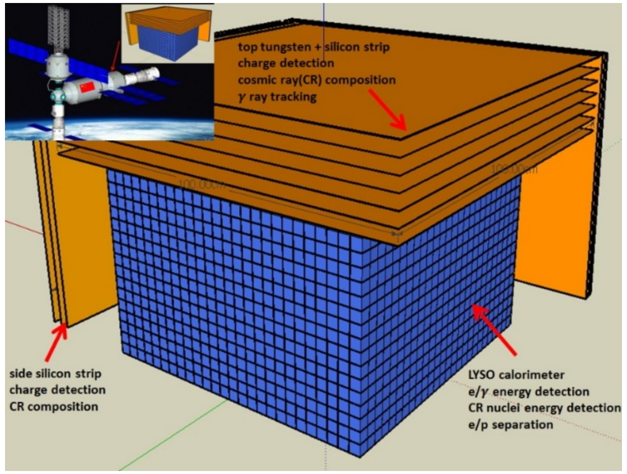

HERD LYSO Calorimeter in space

Can we afford?

Cost-Effective Sapphire Crystals for HHCAL

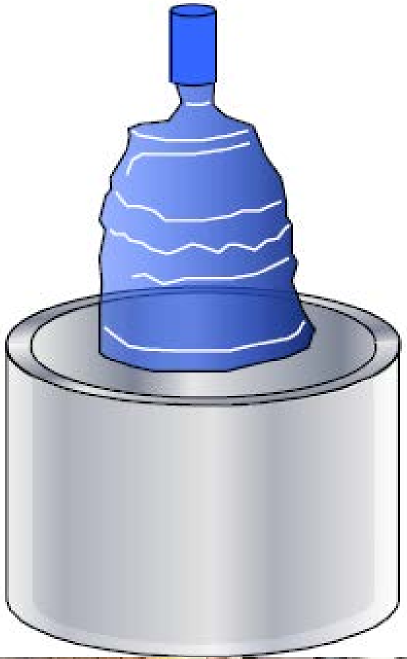

With Kyropoulos (KY) growth technology mass production capability of Sapphire crystal exists
A typical producer can grow 1,000 tons of Sapphire ingots annually with 400 to 450 kg/ingot
The mass production cost of undoped Sapphire crystals after processing is less than $1/cc

Sapphire Crystal	Weight (g)	Size (cm)	Unit Price	Comment
Ingot Boule	400,000	Φ50×55	US$12,000/pc	Undoped
Cutting/Polishing	4	1×1×1	**~US$0.6/cc**	Undoped

Preliminary Result of Ti-Sapphire Crystals

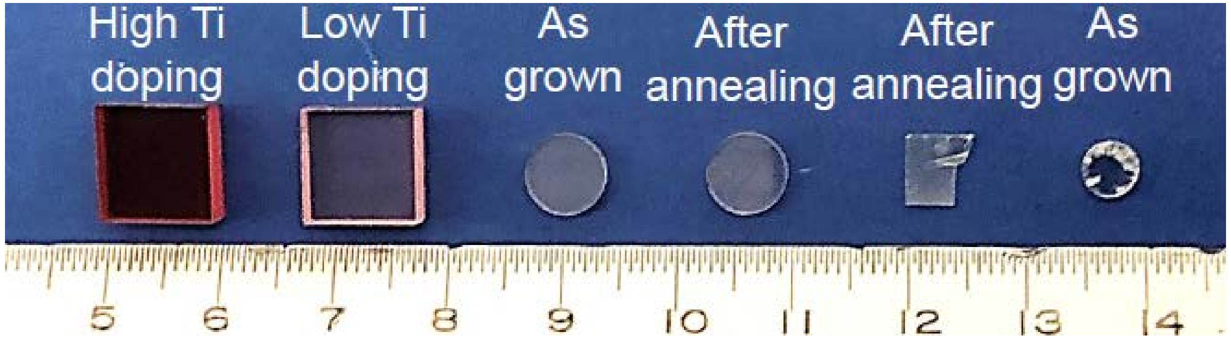

Ti:Sapphire crystals show a weak emission at 325 nm with 150 ns decay time and a strong emission at 755 nm with 3 µs decay time. The latter may be used for the HHCAL concept.

ID	Dimension (mm³)	#	Polishing
Al_2O_3:Ti-1,2	10×10×4	2	Two faces
Al_2O_3:C-1,2	Φ7×1	2	Two faces
Lu_2O_3:Yb	6.4×4.8×0.4	1	Two faces
$LuScO_3$:Yb	Φ4.8×1.3	1	Two faces
All samples received on April 15st 2019 (Monday)			

X-Luminescence

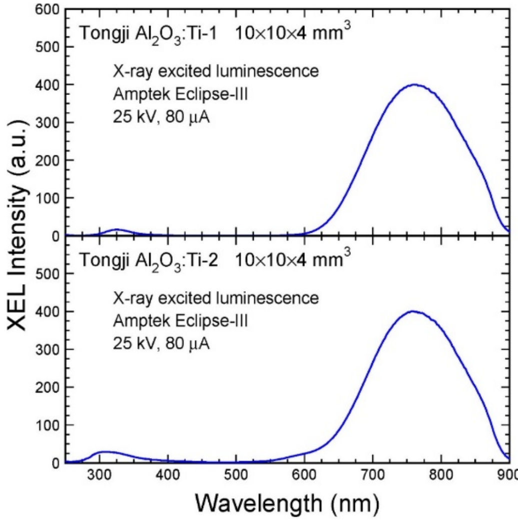

Photo-Luminescence 1

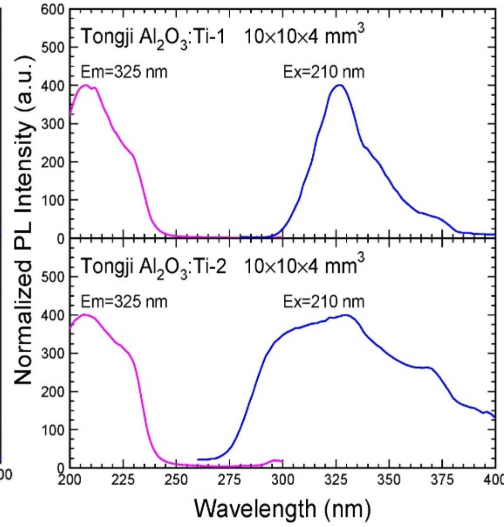

Photo-Luminescence 2

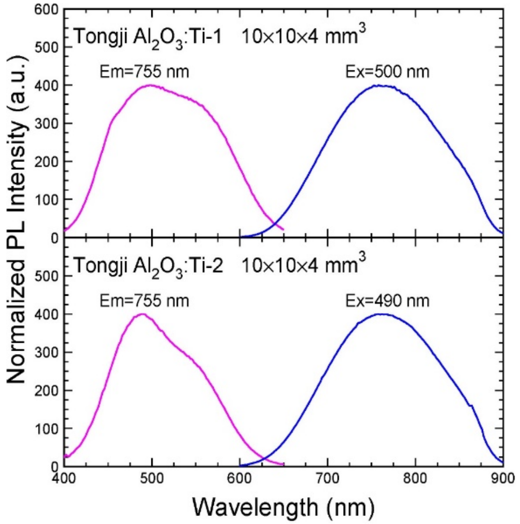

Decay Luminescence 1

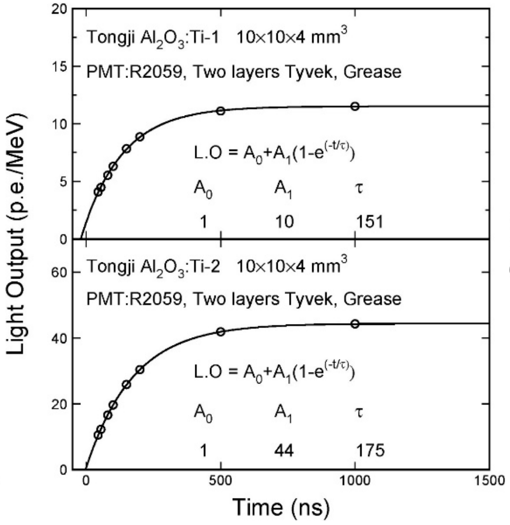

Decay Luminescence 2

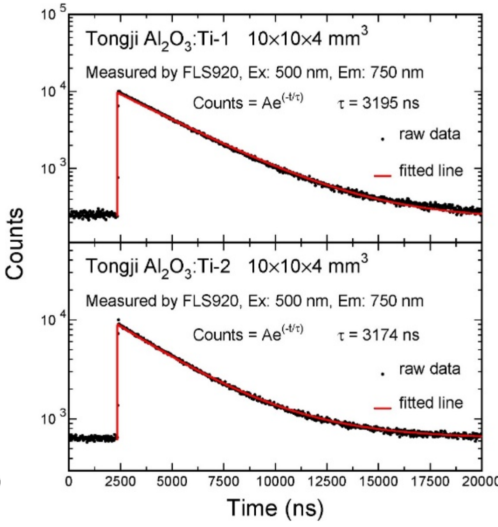

Summary

- LYSO crystals are radiation hard for applications at the HL-LHC, such as CMS BTL. BaF_2 shows a radiation hardness similar to LYSO at high radiation dose. LuAG:Ce ceramics may provide an alternative of LYSO, provided that its slow component is eliminated.
- Commercially available undoped BaF_2 crystals provide ultrafast light with sub-ns decay time. Yttrium doping in BaF_2 crystals increases its F/S ratio significantly while maintaining the intensity of the sub-ns fast component. With a sub-ns pulse width BaF_2:Y promises an ultrafast calorimetry to cope with unprecedented event rate. Large size BaF_2:Y samples show significantly improved optical quality.
- Mass production capability of Sapphire crystals exists with a cost of less than $1/cc. Ti-Sapphire crystals show a scintillation at 755 nm with 3 μs decay time and a cut-off wavelength at 280 nm, which may be used to construct an HHCAL with dual readout of both scintillation and Cerenkov light.
- Additional ultrafast scintillators under development are ZnO:Ga films, quantum confinement based all inorganic Cs Pb halide perovskite QD.

Acknowledgements: DOE HEP Award DE-SC0011925

All Inorganic Cs Pb Halide Perovskite QD

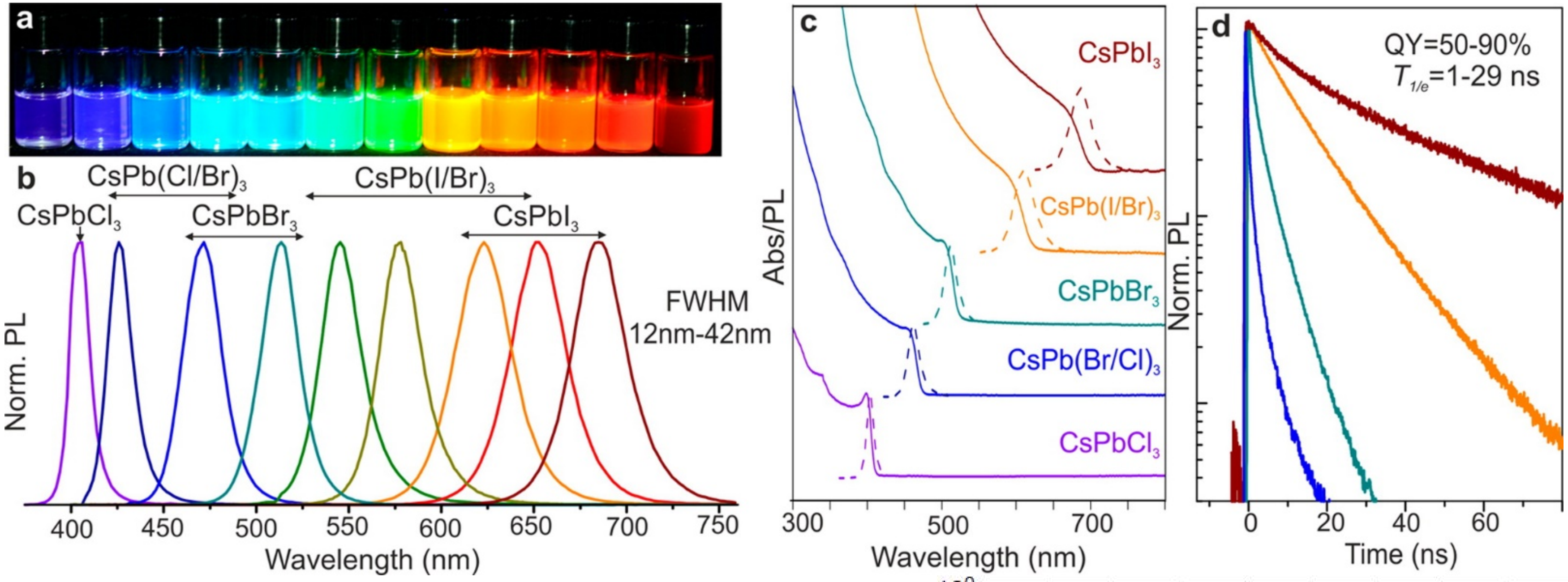

2015 | VOL 15 | Nano Lett. | 3692-3696

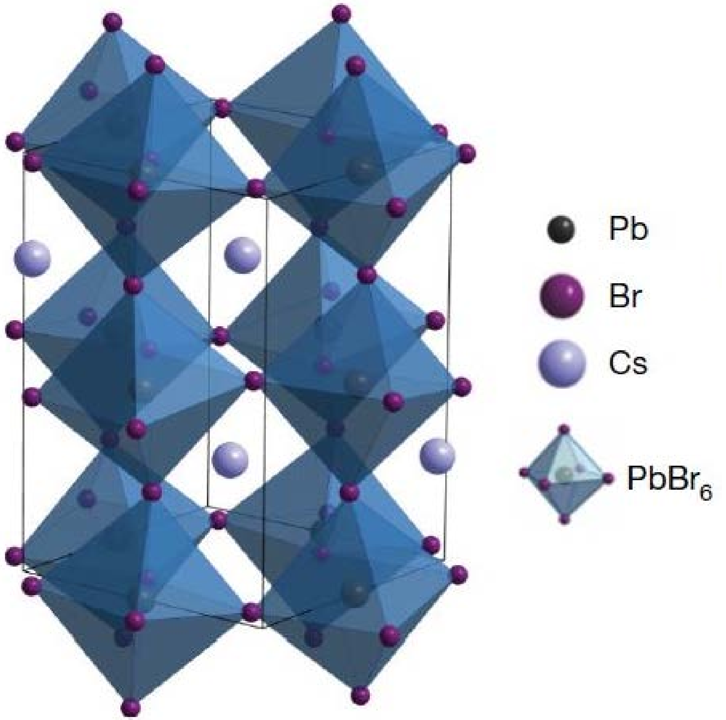

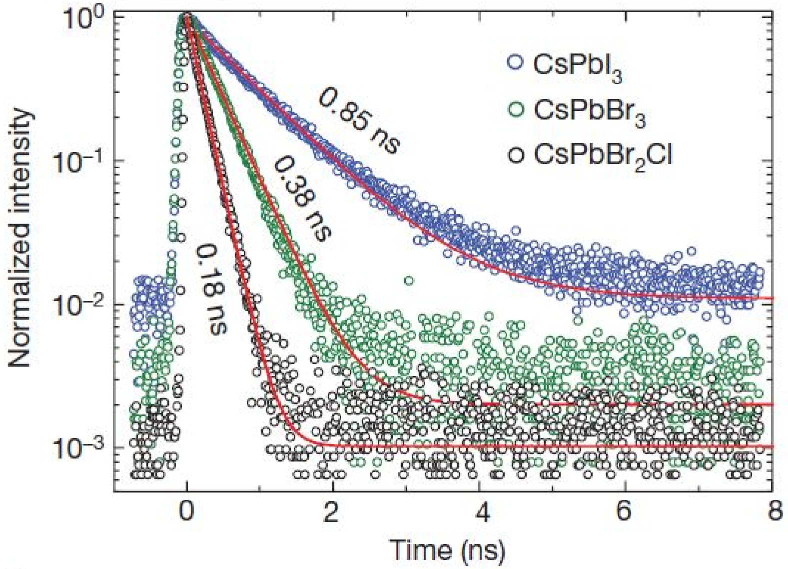

Absorption, emission wavelength and decay time can be tuned for size and composition with quantum efficiency up to 90%.

11 january 2018 | VOL 553 | Nature | 189

Diamond Photodetector

E. Monroy, F. Omnes and F. Calle,"Wide-bandgap semiconductor ultraviolet photodetectors, IOPscience 2003 Semicond. Sci. Technol. 18 R33

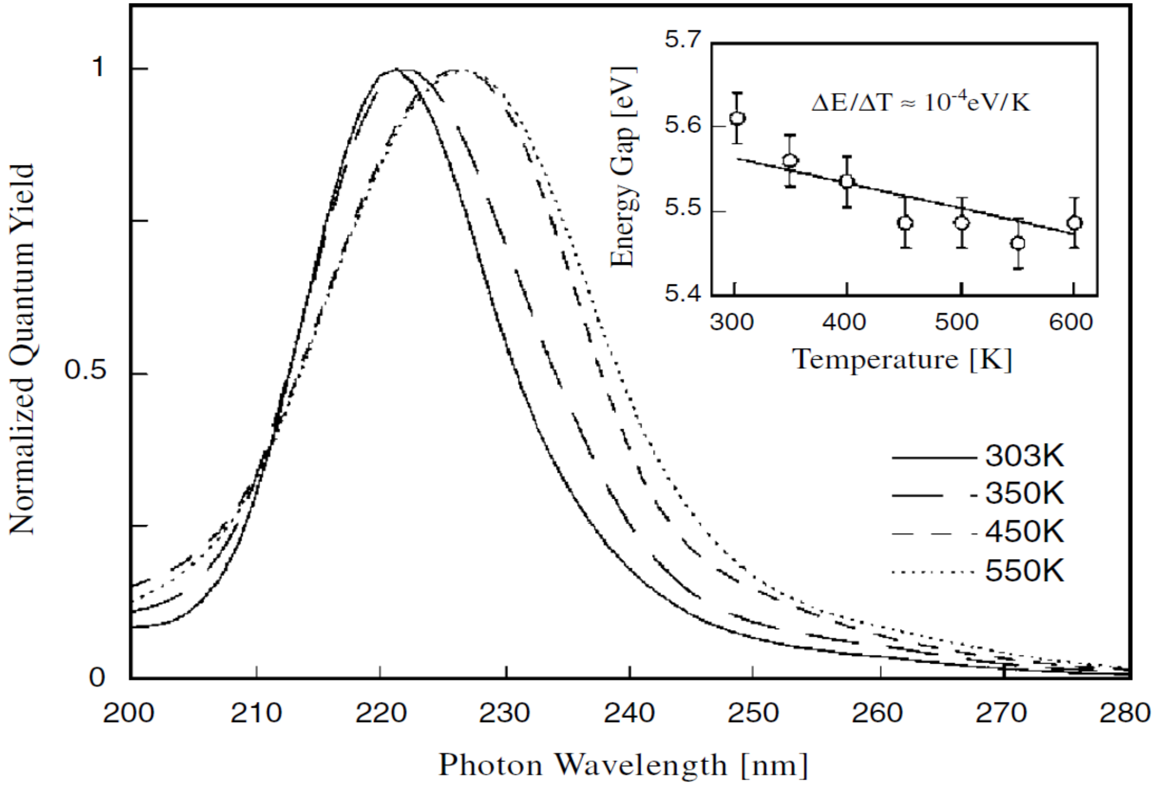

Figure 6. Quantum efficiency of diamond photoconductors at different temperatures and Arrhenius plot of the peak value (inset). (From [Sal00].)

E. Pace and A. De Sio, "Innovative diamond photo-detectors for UV astrophysics", Mem. S.A.It. Suppl. Vol. 14, 84 (2010)

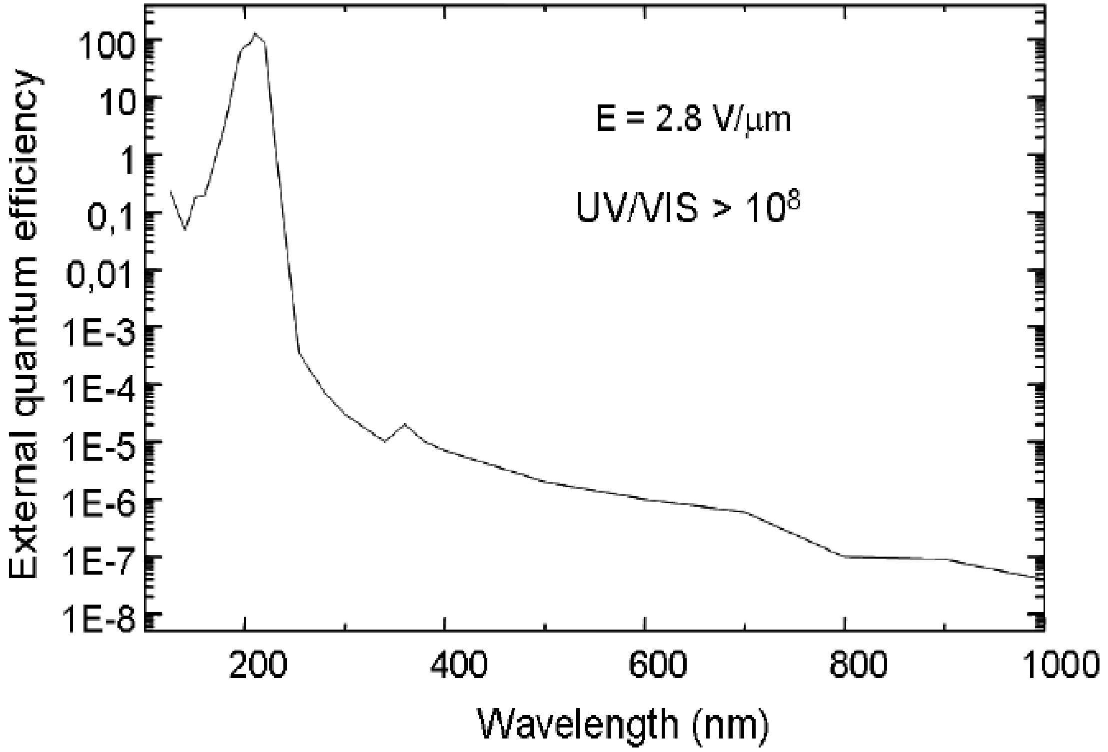

Fig. 4. External quantum efficiency extended to visible and near infrared wavelength regions. The

Properties of Heavy Crystal with Mass Production Capability

Crystal	NaI:Tl	CsI:Tl	CsI	BaF_2	CeF_3	PbF_2	BGO	BSO	$PbWO_4$	LYSO:Ce	AFO Glasses	Sapphire:Ti
Density (g/cm^3)	3.67	4.51	4.51	4.89	6.16	7.77	7.13	6.8	8.3	7.40	4.6	3.98
Melting points (°C)	651	621	621	1280	1460	824	1050	1030	1123	2050	\	2040
X_0 (cm)	2.59	1.86	1.86	2.03	1.65	0.94	1.12	1.15	0.89	1.14	2.96	7.02
R_M (cm)	4.13	3.57	3.57	3.10	2.39	2.18	2.23	2.33	2.00	2.07	2.89	2.88
λ_I (cm)	42.9	39.3	39.3	30.7	23.2	22.4	22.7	23.4	20.7	20.9	26.4	24.2
Z_{eff}	50.1	54.0	54.0	51.6	51.7	77.4	72.9	75.3	74.5	64.8	42.8	11.2
dE/dX (MeV/cm)	4.79	5.56	5.56	6.52	8.40	9.42	8.99	8.59	10.1	9.55	6.84	6.75
λ_{peak} [a] (nm)	410	560	420 310	300 220	340 300	\	480	470	425 420	420	365	750
Refractive Index[b]	1.85	1.79	1.95	1.50	1.62	1.82	2.15	2.68	2.20	1.82	\	1.76
Normalized Light Yield[a,c]	120	190	4.2 1.3	42 4.8	8.6	\	25	5	0.4 0.1	100	1.5	\
Total Light yield (ph/MeV)	35,000	58,000	1700	13,000	2,600	\	7,400	1,500	130	30,000	450	\
Decay time[a] (ns)	245	1220	30 6	600 0.5	30	\	300	100	30 10	40	40	3200
Hygroscopic	Yes	Slight	Slight	No	No	No	No	No	No	No	No	No
Experiment	Crystal Ball	CLEO BaBar BELLE BES III	KTeV	TAPS	\	A4	L3 BELLE	\	CMS ALICE PrimEx Panda	SuperB HL-LHC	\	\